SUPPLEMENTAL DATA

SUPPLEMENTAL MATERIALS AND METHODS

Sample Processing

Peripheral blood mononuclear cells (PBMCs) were purified with Histopaque (Sigma-Aldrich) by density gradient separation. Freshly resected human glioblastoma tissue was minced into small pieces using a scalpel, dissociated using a Pasteur pipette, and suspended in RPMI 1640 medium containing Liberase TM Research Grade Enzyme (Roche) at a final concentration of 30 μg/ml. The prepared mixture was incubated for 1 hour at 37°C with agitation. After brief centrifugation, the pellet was resuspended in 20 ml of 1.03 Percoll (GE Healthcare) underlayed with 10 ml of 1.095 Percoll, and overlayed with 10 ml of 5% FBS in PBS (Hyclone). The tube was centrifuged at 1,200 *g* for 20 minutes at room temperature with no brake. After centrifugation, the cell layer on top of the 1.095 Percoll was collected, filtered through a 70-μm nylon strainer (BD Biosciences), washed and cells were counted using a cellometer (Nexelom Bioscience, Lawrence, MA). NK cells were magnetically purified using NK cells isolation kit (Miltenyi).

NK cell expansion

NK cells were purified from PBMCs from healthy donors using an NK cell isolation kit (Miltenyi Biotec, Inc., San Diego, CA, USA). NK cells were stimulated with irradiated (100 Gy) K562-based feeder cells engineered to express 4-1BB ligand and CD137 ligand (referred to as Universal APC) at a 2:1 feeder cell:NK ratio and

recombinant human IL-2 (Proleukin, 200 U/ml; Chiron, Emeryville, CA, USA) in complete CellGenix GMP SCGM Stem Cell Growth Medium (CellGenix GmbH, Freiburg, Germany) on day 0. After 7 days of expansion, NK cells were used for *in vivo* mice experiments and for *in vitro* studies.

Antibodies used for flow cytometry

Surface antibodies (NK cell phenotype): CD2- PE-Cy7 (clone RPA-2.10; cat# 300222), CD3-APC-Cy7 (clone SK7; cat# 344818), CD56-BV605 (clone HCD56; cat# 318334), CD16- BV650 (clone 3G8; cat# 302042), NKp30-biotin (clone P30-15; cat# 325206), DNAM-FITC (clone TX25; cat# 337104), 2B4- PE (clone C1.7; cat# 329508), NKG2D-PE (clone 1D11; cat# 320806), Siglec-7-PE (clone S7.7; cat# 347703), Siglec-9-PE (clone K8; cat# 351504), PD-1-BV421 (clone 29F.1A12; cat# 135218), CD103-PE-Cy7 (clone 2E7; cat# 121426), CD62L-PE-Cy7 (clone MEL-14; cat# 104418), CCR7-FITC (clone G043H7; cat# 353216), CXCR1-APC (clone 8F1/CXCR1; cat# 320612), CX3CR1-PE-cy7 (clone SA011F11; cat# 149016), CXCR3-PerCP-Cy5.5 (clone G025H7; cat# 353714) (Biolegend), NKp44-PerCP eflour710 (clone 44.189; cat# 46-3369-42) and TIGIT-APC (clone MBSA43**;** cat# 17-9500-42) (eBiosciences/Thermo-Fisher Scientific), streptavidin-BV785 (cat# 563858), PD-1-BV421 (clone EH12.1; cat# 562516), CD9-V450 (clone M-L13; cat# 561326) and NKp46-BV711 (clone 9E2; cat# 563043) (BD Biosciences), Human KIR-FITC (clone 180704; cat# MAB1848) and NKG2C-APC (clone 134591; cat# FAB138A-100) (R&D), NKG2A-PE-Cy7 (clone Z199; cat# IM3291U) and ILT2-APC (clone HP-F1; cat# B30645) (Beckman

Coulter) and CD57-PerCP (clone TB01; cat# NBP2-62203PCP) (Novus Biological).

Intracellular antibodies (NK cell phenotype): Ki-67-PE (clone 16A8; cat# 652404) and t-bet-BV711 (clone 4B10; cat# 644820) (Biolegend), Eomesodermin-eFluor660 (clone WD1928; cat# 50-4877-42) and SAP-PE (clone XLP-1D12; cat# 12-9787-42) (eBiosciences), Granzyme-PE-CF594 (clone GB11; cat# 562462) (BD Biosciences), DAP12-PE (clone 406288; cat# IC5240P) (R&D) and DAP10-FITC (polyclonal; cat# bs-15430R-FITC) (Bioss Antibodies).

Surface antibodies (GSC phenotype): MICA/B-PE (clone 6D4; cat# 320906), CD155-PE-Cy7 (clone SKII.1; cat# 337614), CD112-PE (clone TX31; cat# 337414), HLA-E-PE (clone 3D12; cat# 342604) and HLA-ABC-APC (clone W5/32; cat# 311410) (Biolegend), ULBP1-APC (clone 170818; cat# FAB1380A), ULBP2/5/6-APC (clone 165903; cat# FAB1298A) and ULBP3-PE (clone 166510; cat# FAB1517P) (R&D), HLA-DR-APC (clone L243; cat# 347403) (BD Biosciences) and B7-H6-AF488 (polyclonal; bs-12559R-A488) (Bioss antibodies).

GBM-TCGA RNA dataset analysis

The TCGA GBM molecular subtype information were retrieved from R package TCGAbiolinks as originally identified by Verhaak et al. (1-3). To quantify the NK cell abundance relative to total immune cell content within each tumor sample, we downloaded the CIBERSORT results of 22 immune cell types for TCGA GBM from Thorssen et al. (4). The Wilcoxon test was used to compare the NK abundance

between each subtype, and the p values were adjusted by Benjamini-Hochberg procedure.

NK cell cytotoxicity assays

NK cells were co-cultured for 5 hours with K562 or GSCs target cells at an optimized effector:target ratio of 5:1 together with CD107a PE-CF594 (clone H4A3; cat# 562628) (BD Biosciences), monensin (BD GolgiStopTM) and BFA (Brefeldin A, Sigma Aldrich). NK cells were incubated without targets as the negative control and stimulated with PMA (50 ng/mL) and ionomycin (2 mg/mL, Sigma Aldrich) as positive control. Cells were collected, washed and stained with surface antibodies (mentioned above), fixed/permeabilized (BD Biosciences) and stained with IFN-γ v450 (clone B27; cat# 560372) and TNF-α Alexa700 (clone MAb11; cat# 557996) (BD Biosciences) antibodies.

Chromium release assay

NK cell cytotoxicity was assessed using chromium (^{51}Cr) release assay. Briefly, K562 or GSCs target cells were labeled with ^{51}Cr (PerkinElmer Life Sciences, Boston, MA) at 50 μCi/5 × 10^5 cells for 2 hours. ^{51}Cr-labeled K562/GSC targets (5 × 10^3) were incubated for 4 h with serially diluted magnetically isolated NK cells in triplicate. Supernatants were then harvested and analysed for ^{51}Cr content.

Incucyte live imaging

After co-culture with GSCs, NT NK cells and *TGFBR2* KO NK cells were purified and labeled with Vybrant DyeCycle Ruby Stain (ThermoFisher) and co-cultured at a 1:1 ratio with K562 targets labeled with CellTracker Deep Red Dye (ThermoFisher). Apoptosis was detected using the CellEvent Caspase-3/7 Green Detection Reagent (ThermoFisher). Frames were captured over a period of 24 hrs at 1 hour intervals from 4 separate 1.75 x 1.29 mm^2 regions per well with a 10× objective using IncuCyte S3 live-cell analysis system (Sartorius). Values from all four regions of each well were pooled and averaged across all three replicates. Results were expressed graphically as percent cytotoxicity by calculating the ratio of red and green overlapping signals (count per image) divided by the red signal (counts per image).

Suppression assay

For studies of NK cell suppression by GSCs and human astrocytes, magnetically selected healthy NK cells were cultured in Serum-free Stem Cell Growth Medium (SCGM; CellGro /CellGenix) supplemented with 5% glutamine, 5 μM HEPES (both from GIBCO/ Invitrogen), and 10% FCS (Biosera) in 96-well flat-bottomed plates (Nunc) at 100,000/100μl. NK cells were co-cultured either alone (positive control) or with GSCs or astrocytes at a 1:1 ratio for 48 hours at 37 °C before performing functional assays to assess NK cells cytotoxicity.

Functional assays for blocking NK cytotoxicity

Magnetically purified NK cells were cultured alone or with blocking antibodies against NKG2D (clone 1D11; cat# 320802), DNAM (clone 11A8; cat# 338302) and NKp30 (clone P30-15; cat# 325223) (Biolegend) overnight (5 µg/ml). ^{51}Cr release assay was then performed as described above. For HLA-KIR blocking, GSCs were cultured alone or with an HLA-ABC blocking antibody (clone W6/32, Biolegend; cat# 311402) before performing ^{51}Cr release assay.

NK cell functional assays

GSCs and purified NK cells were co-cultured for 48 hours in the presence of anti–TGFβ 123 (5 µg/ml) (clone 1D11; cat# MAB1835-500, R&D), HLA-ABC blocking antibody (clone W6/32; cat# 311402, Biolegend), CD44 blocking antibody (clone IM7; cat# 103002, Biolegend), ILT-2 (CD85J) blocking antibody (clone HP-F1; cat# 16-5129-82**,** ThermoFisher), CD155 blocking antibody (clone D171; cat# GTX72348, GenTex), CD112 blocking antibody (clone TX31; cat# 337402, Biolegend), 10 µM LY2109761, 10 µM galunisertib (LY2157299), 10 µM Cilengitide (Cayman Chemical) or 1 µM MMP-2/MMP-9 inhibitor I (Millipore). Cytotoxicity assays were then performed as described above.

NK cell recovery assays

NK cells were cultured either with GSCs in a 1:1 ratio or alone for 48 hours. After 48 hours of co-incubation, NK cells were then either purified again by bead selection and resuspended in SCGM media or remained in culture with GSCs for an additional 48 hours and then used for ^{51}Cr release assay. In a second assay,

after reselection, NK cells were cultured for another 5 days in SCGM in the presence of 5 ng/ml IL-15 with or without 10μM galunisertib before use for ^{51}Cr release assay.

Mass cytometry

Sample preparation, staining and acquisition

NK cells were harvested, washed twice with cell staining buffer (0.5% bovine serum albumin/PBS) and incubated with 5 μl of human Fc receptor blocking solution (Trustain FcX, Biolegend, San Diego, CA) for 10 minutes at room temperature. Cells were then stained with a freshly prepared CyTOF antibody mix against cell surface markers as described previously (5, 6). Samples were acquired at 300 events/second on a Helios instrument (Fluidigm) using the Helios 6.5.358 acquisition software (Fluidigm). Mass cytometry data were normalized based on EQ^{TM} four element signal shift over time using the Fluidigm normalization software 2. Initial data quality control was performed using Flowjo version 10.2. Calibration beads were gated out and singlets were chosen based on iridium 193 staining and event length. Dead cells were excluded by the Pt195 channel and further gating was performed to select CD45+ cells and then the NK cell population of interest (CD3-CD56+). A total of 320,000 cells were proportionally sampled from all samples to perform automated clustering

Data Analysis

The mass cytometry data were merged together using Principal Component Analysis (PCA), “RunPCA” function, from R package Seurat (v3). Dimensional reduction was performed using “RunUMAP” function from R package Seurat (v3) with the top 20 principal components. The UMAP plots were generated using the R package ggplot2 (v3.2.1). Data were analyzed using automated dimension reduction including (viSNE) in combination with FlowSOM for clustering (7) for the deep phenotyping of immune cells as published before _ENREF_47(8). We further delineated relevant cell clusters, using our in-house pipeline for cell clustering. To generate the heatmap, CD45+CD56+CD3- gated FCS files were exported from FlowJo to R using function “read.FCS” from the R package flowCore (v3.10). The markers expression was transformed using acrsinh with a cofactor of 5. The mean values of 36 markers were plotted as heat map using the function “pheatmap” from R package pheatmap (v1.0.12). Markers with similar expression were hierarchically clustered.

Single cell RNA sequencing

Gliomas were mechanically dissociated with scissors while suspended in Accutase solution (Innovative Cell Technologies, Inc.) at room temperature and then serially drawn through 25-, 10- and 5-mL pipettes before being drawn through an 181/2-gauge syringe. After 10 minutes of dissociation, cells were spun down at 420 x g for 5 minutes at 4°C and then resuspended in 10 mL of a 0.9N sucrose solution and spun down again at 800 x g for 8 minutes at 4°C with the brake off. Once sufficient samples were accumulated to be run in the 10x pipeline (10x Genomics;

6230 Stoneridge Mall Road, Pleasanton, CA 94588), cells were then thawed and resuspended in 1 mL of PBS containing 1% BSA, for manual counting. Cells were then stained with the CD45 antibody (BD Biosciences, San Jose, CA, cat #: 555482) at 1:5 for 20 minutes on ice. Samples had Sytox blue added just before sorting so that only live CD45+ cells would be collected. Cells were then sorted in a solution of 50% FBS and 0.5% BSA in PBS, spun down, and resuspended at a concentration of 700-1200 cells/μL for microfluidics on the 10x platform (10x Genomics). The 10x protocol, which is publicly available, was followed to generate the cDNA libraries that were sequenced. (https://assets.ctfassets.net/an68im79xiti/2NaoOhmA0jot0ggwcyEKaC/fc58451fd97d9cbe012c0abbb097cc38/CG000204_ChromiumNextGEMSingleCell3_v3.1_Rev_C.pdf). The libraries were sequenced on an Illumina next-seq 500, and up to 4 indexed samples were multiplexed into one output flow cell using the Illumina high-output sequencing kit (V2.5) in paired-end sequencing (R1, 26nt; R2, 98nt, and i7 index 8nt) as instructed in the 10x Genomics 3' Single-cell RNA sequencing kit. The data were then analyzed using the cellranger pipeline (10x Genomics) to generate gene count matrices. NK markers used for gating included KLRD1, NKG7, and NKTR (9) in both the PBMC and the GBM dataset.

The mkfastq argument (10x Genomics) was used to separate individual samples with simple csv sample sheets to indicate the well that was used on the i7 index plate to label each sample. The count argument (10x Genomics) was then used with the expected number of cells for each patient. The numbers varied between 2,000 and 8,000 depending on the number of viable cells isolated. Sequencing

reads were aligned with GRCh38. The aggr argument (10x Genomics) was then used to aggregate samples from each patient for further analysis. Once gene-count matrices were generated, they were read into an adapted version of the Seurat pipeline for filtering, normalization, and plotting. Genes that were expressed in less than three cells were ignored, and cells that expressed less than 200 genes or more than 2500 genes were excluded, to remove potentially poor- and high-PCR artifact cells, respectively. Finally, to generate a percentage of mitochondrial DNA expression and to exclude any cells with more than 25% mitochondrial DNA (as these may be doublets or low-quality dying cells), cells were normalized using regression to remove the percent mitochondrial DNA variable via the scTransform command which corrects for batch effects as well. Datasets were then processed for principal component analysis (PCA) with the RunPCA command, and elbow plots were printed with the ElbowPlot command in order to determine the optimal number of PCs for clustering; 15 PCs were chosen for this analysis. Next, the cell clusters were identified and visualized using SNN and UMAP, respectively, before generating a list of differentially-expressed genes for each cluster. A list of differentially-expressed genes was generated to label our clusters at low resolution (0.1). These clusters' labels were based on at least three differentially-expressed genes, and violin plots were generated to show the relative specificity to the cluster. Differentially-expressed genes were identified using cutoffs for min.pct = 0.25 and logfc.threshold = 0.25. Plots were generated with either the DimPlot, FeaturePlot or VlnPlot commands. Next we identified the clusters containing NK cell populations in both the PBMC and GBM dataset: NK markers included KLRD1,

NKG7, and NKTR(9). Analyses performed on the combination of PBMC and GBM NK cells, were joined using the FindIntegrationAnchors command to determine genes that can be used to integrate the two datasets—after the determination of the Anchors we used the IntegrateData command to combine our two datasets. Data were then normalized using the scTransform command. Datasets were then processed for PCA with the RunPCA command, and elbow plots were printed with the ElbowPlot command in order to determine the optimal number of PCs for clustering, 15 PCs were chosen for this analysis. Next, the cell clusters were identified and visualized using SNN and UMAP, respectively, before generating a list of differentially-expressed genes for each sample. Plots were generated with either the DimPlot, FeaturePlot or VlnPlot commands.

Phospho-Smad2/3 assay

NK cells were stained with Live/dead-aqua and CD56 ECD (Beckman Coulter) for 20 min in the dark at RT, washed with PBS fixed for 10 min in the dark. After one wash, the cells were permeabilized (Beckman Coulter kit) and stained with p-(S465/S467)-Smad2/p-(S423/S425)/Smad3-Alexa 647 mAb Phosflow antibody (clone O72-670; cat# 562696, BD Biosciences) for 30 minutes at room temperature. Cells incubated with 10ng/ml recombinant TGF-β for 45 minutes in 37°C were used as positive control.

MMP2 and MMP9 intracellular staining

NK cells and GSCs were either cultured alone, in a transwell chamber or together in the presence or absence of TGF-β blocking antibodies (clone 1D11; cat# MAB1835-500, R&D) for 48 hours. BFA was added for the last 12 hours of culture. Cells were then fixed/permeabilized (BD Biosciences) and stained with anti-MMP2-PE (clone 1A10; cat# IC9023P, R&D) and MMP9-PE (clone D6O3H; cat# 27647S, Cell Signalling) for 30 minutes before acquisition of data by flow cytometry. The surface markers CD133, CD3 and CD56 were used to distinguish NK cells and GSCs for data analysis.

Reverse transcriptase–polymerase chain reaction (RT-PCR), and quantitative real-time PCR (qPCR)

RNA was isolated using RNeasy isolation kit (Qiagen). A 1 µg sample of total RNA was reverse transcribed to complementary DNA using the iScript cDNA Synthesis Kit (Bio-Rad) according to the manufacturer's instructions. Then, an equivalent volume (1 µL) of complementary DNA (cDNA) was used as a template for quantitative real-time PCR (qPCR) and the reaction mixture was prepared using iTaq™ Universal SYBR® Green Supermix (Biorad) according to the manufacturer's instructions. Gene expression was measured in a StepOnePlus™ (Applied Biosystem) instrument according to the manufacturer's instruction with the following gene-specific primers: *TGFB1* (forward, 5'-AACCCACAACGAAATCTATG-3'; reverse, 5'-CTTTTAACTTGAGCCTCAGC-3'); and *18S* (forward, 5'- AACCCGTTGAACCCCATT -3'; reverse, 5'-CCATCCAATCGGTAGTAGCG -3'). The gene expression data were quantified

using the relative quantification (ΔΔCt) method, and 18S expression was used as the internal control.

CRISPR gene editing of primary NK cells and GSCs

crRNAs were ordered from IDT (www.idtdna.com/CRISPR-Cas9) in their proprietary Alt-R format. Alt-R crRNAs and Alt-R tracrRNA were re-suspended in nuclease-free duplex buffer (IDTE) at a concentration of 200 µM. Equal amount from each of the two RNA components was mixed together and diluted in nuclease-free duplex buffer at a concentration of 44 µM. The mix was boiled at 95˚C for 5 minutes and cooled down at room temperature for 10 minutes. For each well undergoing electroporation, Alt-R Cas9 enzyme (IDT cat # 1081058, 1081059) was diluted to 36 µM by combining with resuspension buffer T at a 3:2 ratio. The guide RNA and Cas9 enzyme were combined using a 1:1 ratio from each mixture. The mixture was incubated at room temperature for 10–20 minutes. Either a 12 well plate or a 24 well plate was prepared during the incubation period. This required adding appropriate volume of media and Universal APCs (1:2 ratio of effector to target cells) supplemented with 200 IU/ml of IL-2 (for NK cells only) into each well. Target cells were collected and washed twice with PBS. The supernatant was removed as much as possible without disturbing the pellet and the cells were resuspended in Resuspension Buffer T for electroporation. The final concentration for each electroporation was 1.8 µM gRNA, 1.5 µM Cas9 nuclease and 1.8 µM Cas9 electroporation enhancer. The cells were electroporated using Neon Transfection System, at 1600V, 10ms pulse width and 3 pulses with 10ul

electroporation tips (Thermo Fisher Scientific (cat # MPK5000)). After electroporation the cells were transferred into the prepared plate and placed in the 37C incubator. The knockout efficiency was evaluated using flow cytometry 7 days after electroporation. Anti-CD51- PE antibody (Biolegend) was used to verify KO efficacy in GSCs.

Mice brain tissue processing and analysis

Brain tissue from the animals was collected and NK cells were isolated using a percoll (GE Healthcare) gradient fallowing protocol described by Pino et al (10). Briefly, brain tissue was dissociated using a 70 µm cell strainer (Life Science, Durham, NC). Cell suspension was re suspended in a 30% isotonic percoll solution and layer on top of a 70% isotonic percoll solution. Cells were centrifuged at 500G for 30 minutes and 18^{o}C with no brake. 2-3 ml of the 70%- 30% interface was collected in a clean tube and washed with PBS 1X. After this procedure, cells were ready for immunostaining with mouse anti-CD45-AF700 (clone 30-F11; cat# 103127), human anti-CD45-PerCP/C5.5 (clone HI30; cat# 304027), human anti-CD56-BV606 (clone 5.1H11; cat# 362537), human anti-CD3-APC/Cy7 (clone HI3a; cat# 300317), human anti-CD103-BV711 (clone Ber-Act8; cat# 350221), human anti-CD9-BV-510 (clone HI9a; cat# 312107), human anti-CD69-BV780 (clone FN50; cat# 310931), human anti-PD-1-BV-421 (clone EH12.2H7; cat# 329919) and human anti-NKG2D-APC (clone 329919; cat# 320807) all from Biolegend.

Histopathology

Brain tissue specimens from untreated control mice, mice treated with either NK cells alone, cilengitide alone, galunisertib alone or with combination therapy of NK + cilengitide or NK + galunisertib were collected. The specimens were bisected longitudinally and half of each brain was fixed in 10% neutral buffered formalin and were then embedded in paraffin. Formalin-fixed, paraffin embedded tissues were sectioned at 4 μm, and stained routinely with hematoxylin and eosin. Brains were examined for the presence or absence of glioblastoma tumor cells. Sections lacking tumor were also evaluated for evidence of meningoencephalitis using a Leica DM 2500 light microscope by a board-certified veterinary pathologist. One section was examined from each sample. Representative images were captured from comparable areas of cerebral hemispheres with a Leica DFC495 camera using 1.25x, 5x, and 20x objectives.

Granzyme B Immunohistochemical staining

Formalin-fixed, paraffin embedded tissue was routinely sectioned at 4 μm and placed on glass slides. After deparaffinization, Granzyme B staining (human-specific, rabbit monoclonal antibody clone D6E9W, Cell Signaling Technologies) was completed using a Lecia Bond RXm autostainer. Twenty minutes of antigen retrieval in citrate buffer at 95ºC was performed prior to staining. Primary antibody was diluted at 1:100 with an incubation time of 60 minutes. Hematoxylin was used for nuclear counterstain and sections were routinely cover-slipped. Slides were examined using a Leica DM2500 microscope and images were captured at 2.5x, 20x, and 60x using a Leica DMC6200 camera and Leica Application Suite (LAS) software.

SUPPLEMENTAL FIGURES

Supplemental Figure 1

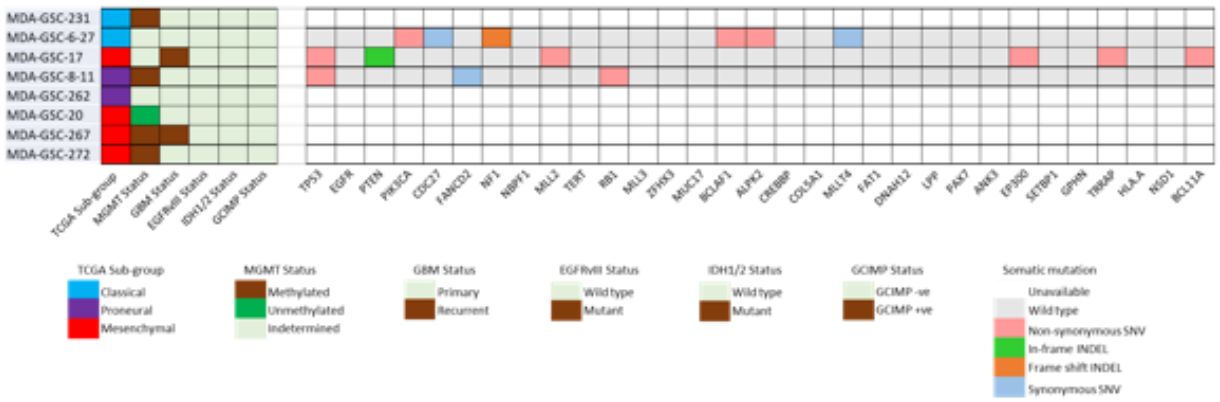

Supplemental Figure 1. Transcriptional profile of the patient-derived GSCs. A comparative heatmap depicting the characteristics of patient-derived GSC cell lines, including their molecular subtypes based on the comprehensive catalogue of the cancer genome atlas (TCGA), MGMT gene promoter methylation status, EGFR variant III (EGFRvIII) and IDH mutation status, and somatic mutation profiling (≥10%). GSC20 and GSC272 were used for the *in vivo* mouse models in our study.

Supplemental Figure 2

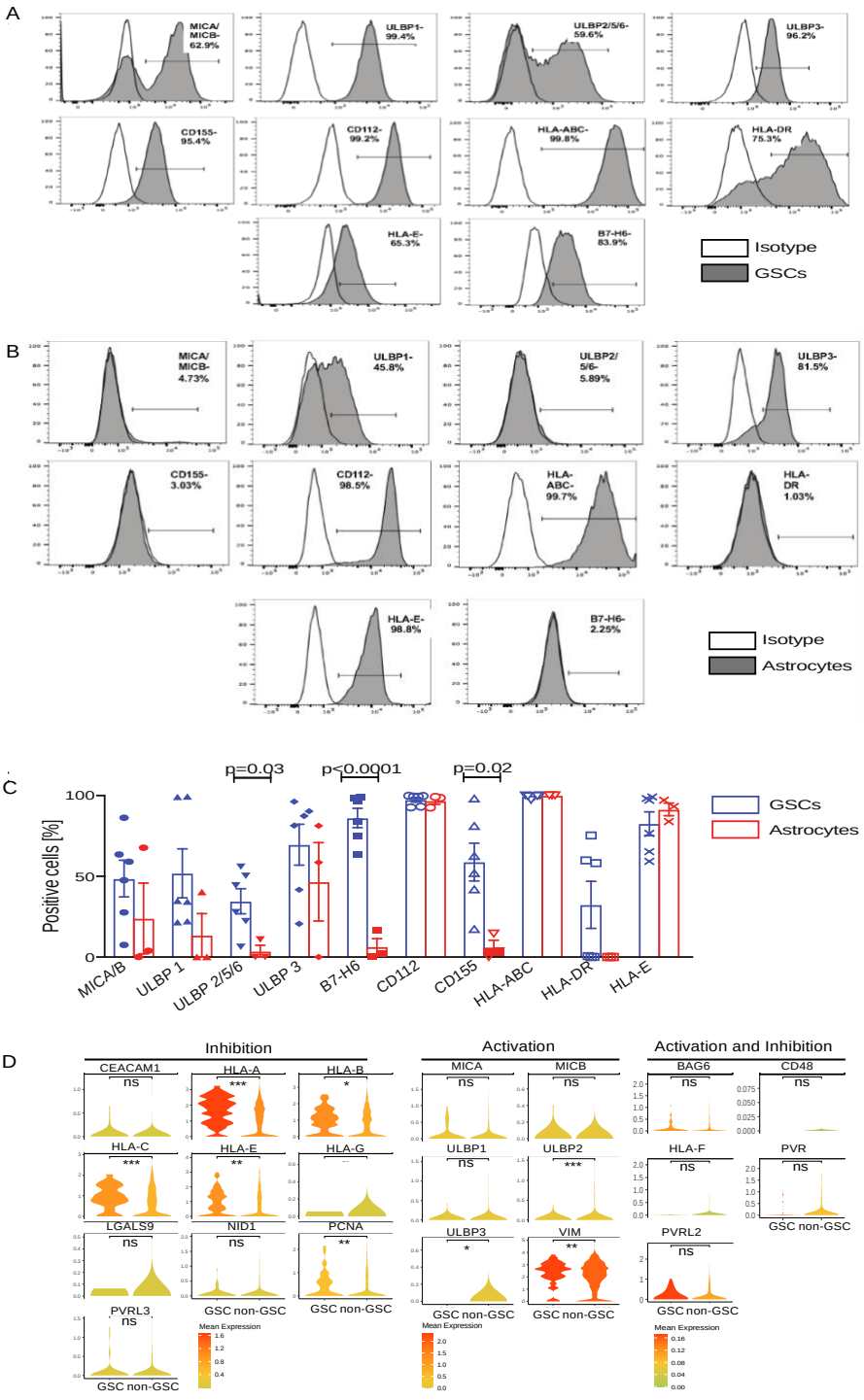

Supplemental Figure 2. Expression of ligands for activating and inhibitory NK cell receptors on GSCs, mature GBM neoplastic cells and healthy astrocytes A, B Representative histograms for the mean fluorescence intensity (MFI) of the major NK cell receptor ligands expressed on GSCs (A) and healthy astrocytes (B). C, Cumulative graph depicting NK cell receptor ligands on GSC vs. healthy human astrocytes (GSC: N=6; Astrocytes: N=3). D, Violin plots comparing the expression levels of ligands for activating and inhibitory NK cell receptors on GSC vs. non-GSC (mature neoplastic GBM cells) using data from The Cancer Genome Atlas (TCGA) database. The violin plots are color-coded from yellow (low) to red (high) to depict the mean expression level for each individual marker gene. Statistical analysis by unpaired t-test (C, D). * $p \leq 0.05$, ** $p \leq 0.01$, *** $p \leq 0.001$. ns, not significant.

Supplemental Figure 3

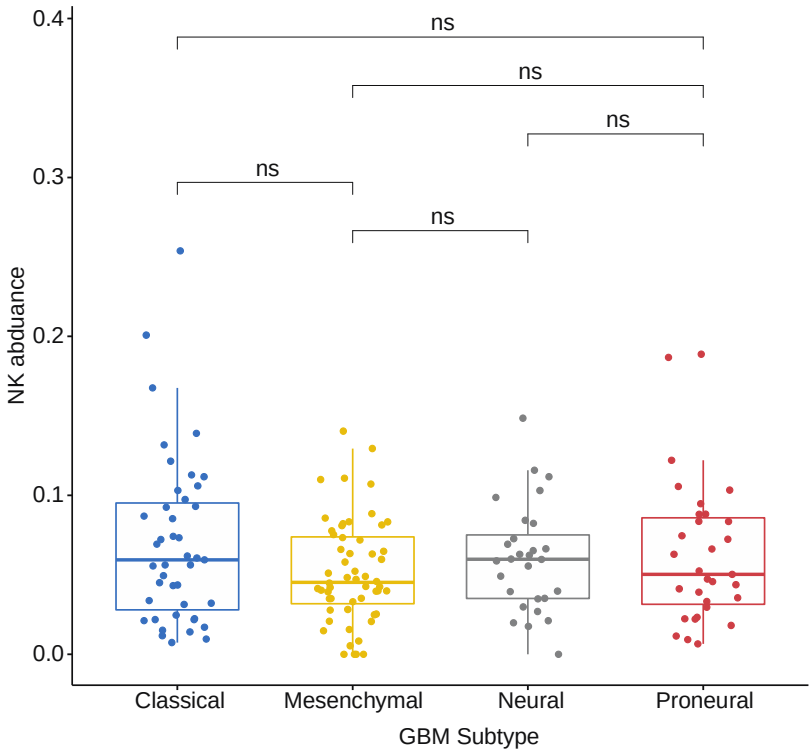

Supplemental Figure 3. NK cells are present in relatively large numbers within the GBM tumor microenvironment. The relative NK cell abundance in the tumor immune microenvironment of the different GBM subtypes was calculated using the publically available GBM-TCGA dataset (classical: n=42, mesenchymal: n=56, neural: n=28, proneural: n=31).

Supplemental Figure 4

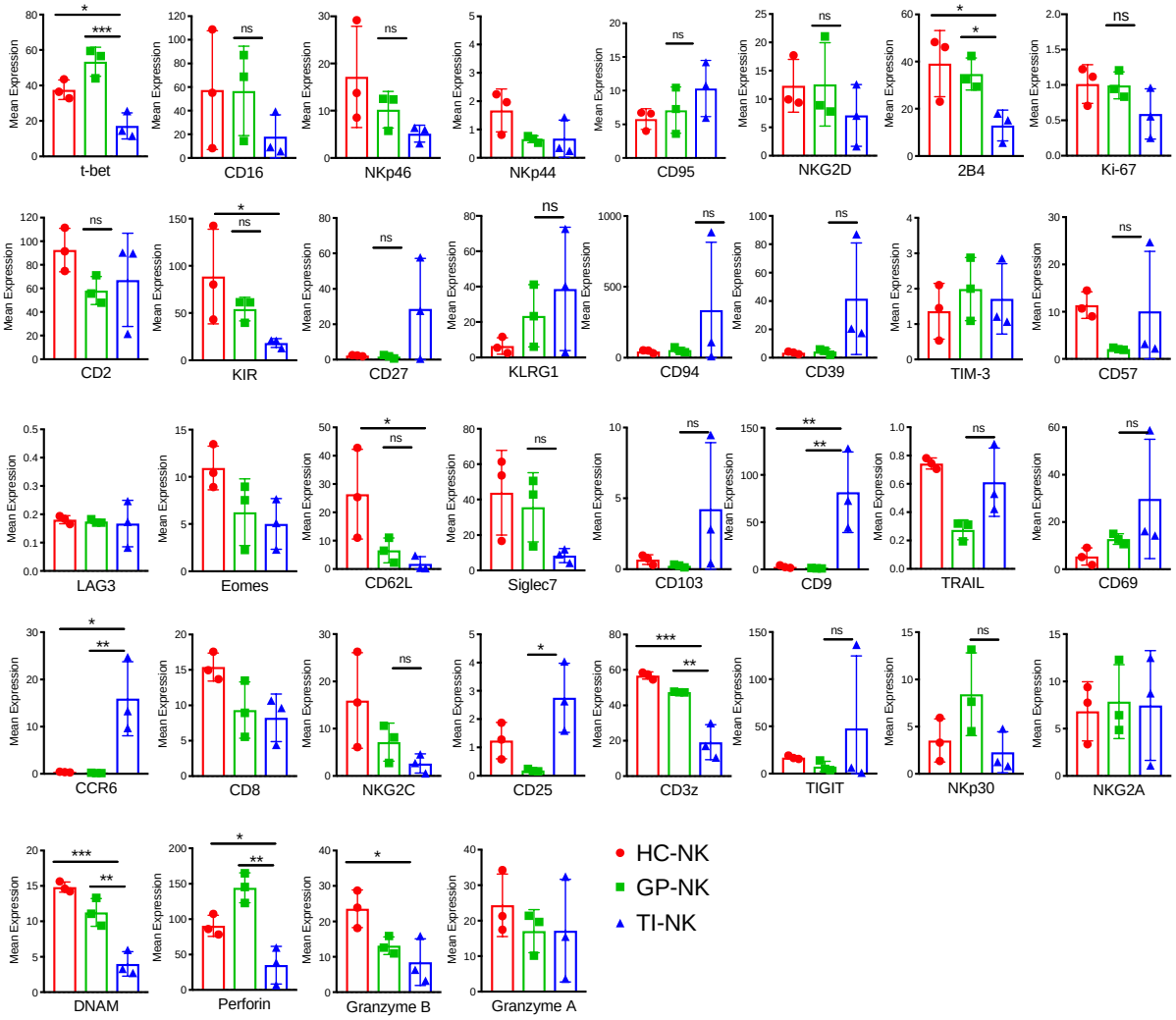

Supplemental Figure 4. GBM tumor infiltrating NK cell phenotype by mass cytometry. Graph summary of mass cytometry data showing the expression of NK cell surface markers, transcription factors and cytotoxicity markers in HC-NK cells (red), peripheral blood NK cells from patients with GBM (GP-NK; green) and TI-NKs (blue). Statistical analysis by repeated measures ANOVA with Dunnett's correction for multiple comparisons. * $p \leq 0.05$, ** $p \leq 0.01$, *** $p \leq 0.001$. ns, not significant.

Supplemental Figure 5

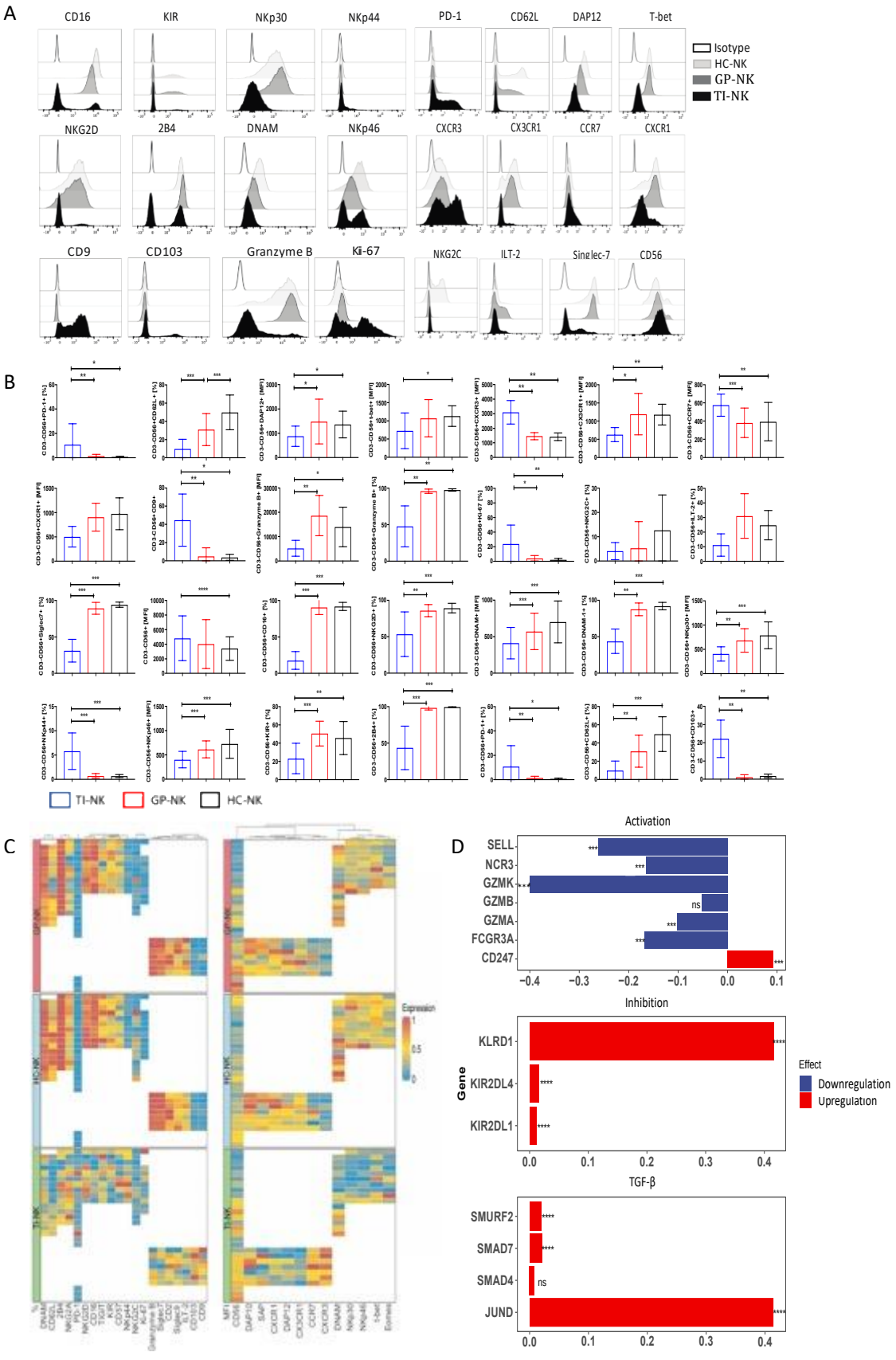

Supplemental Figure 5. Single cell analysis of GBM tumor infiltrating NK cell phenotype and transcriptomic profile. A-C, Multi-parameter flow cytometry data with representative histograms and graph summary for the mean fluorescence intensity (MFI) or frequencies of NK cells expressing individual markers. Comparisons include GBM tumor-infiltrating NK cells (TI-NKs) vs. autologous peripheral blood (GP-NK) from the same patient with GBM vs. peripheral blood from healthy controls (HC-NK). A and B show a selected panel of NK cell markers that were significantly different between TI-NKs and GP-NK or HC-NK as determined by flow cytometry analysis (n=28). C, The color scale of the heatmap represents the expression level for each marker (percentage, right) or MFI (left) ranging from blue (low expression) to red (high expression). The columns represent each marker and the rows represent each patient. D. Bar graphs representing the difference in the average expression of individual genes between TI-NKs and HC-NK. Red indicates that the gene is upregulated in TI-NKs or downregulated in HC-NK cells; blue indicates that the gene is downregulated in TI-NKs or upregulated in HC-NK cells. The genes are divided into 3 groups: activating, inhibitory and TGF-β associated genes. Statistical analysis by repeated measures ANOVA with Dunnett's correction for multiple comparisons (B) or unpaired t-test (D). *p≤ 0.05, **p ≤ 0.01, ***p ≤ 0.001.

Supplemental Figure 6

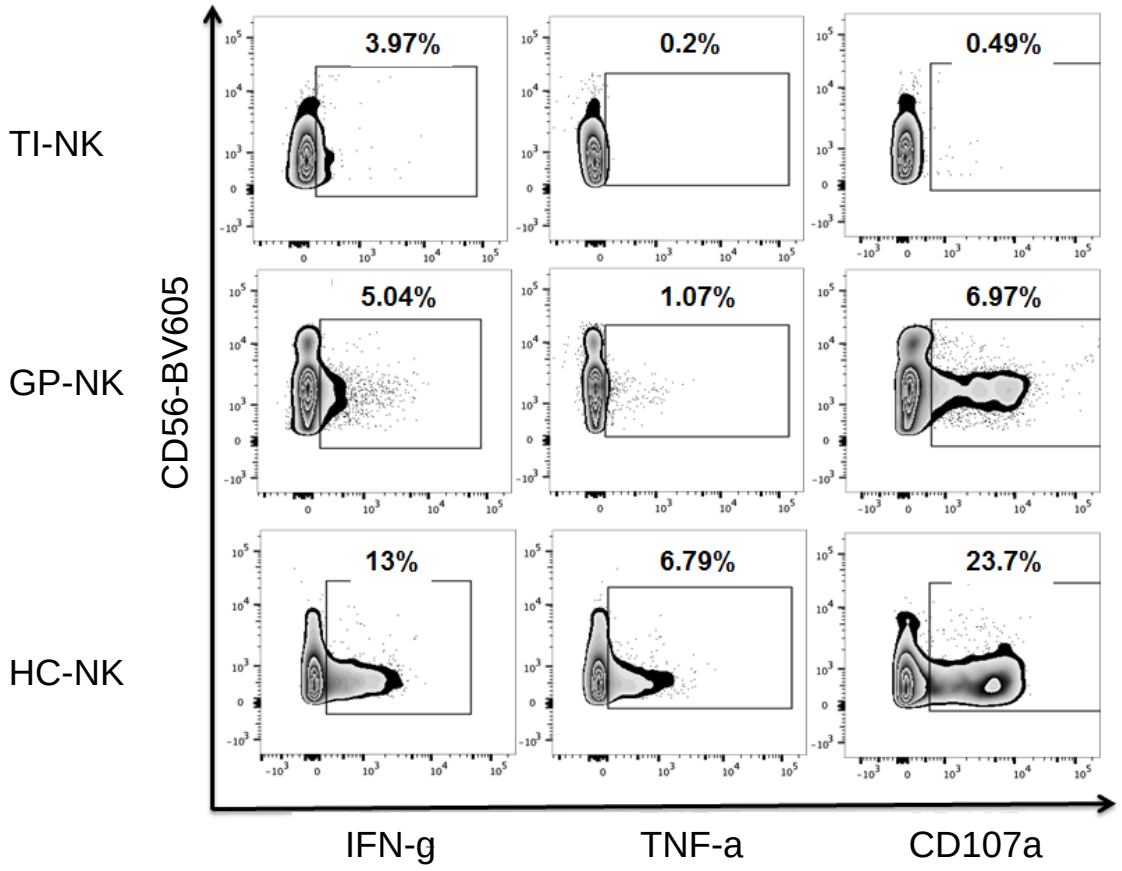

Supplemental Figure 6. GBM TI-NK cells are dysfunctional. Representative zebra plot for CD107a, IFN-γ, and TNF-α production by TI-NKs, GP-NK from patients with GBM or HC-NK cells after incubation with K562 targets for 5 hours at a 5:1 effector:target ratio. Inset numbers are the percentages of CD107a-, IFN-γ- or TNF-α-positive NK cells within the gated populations.

Supplemental Figure 7

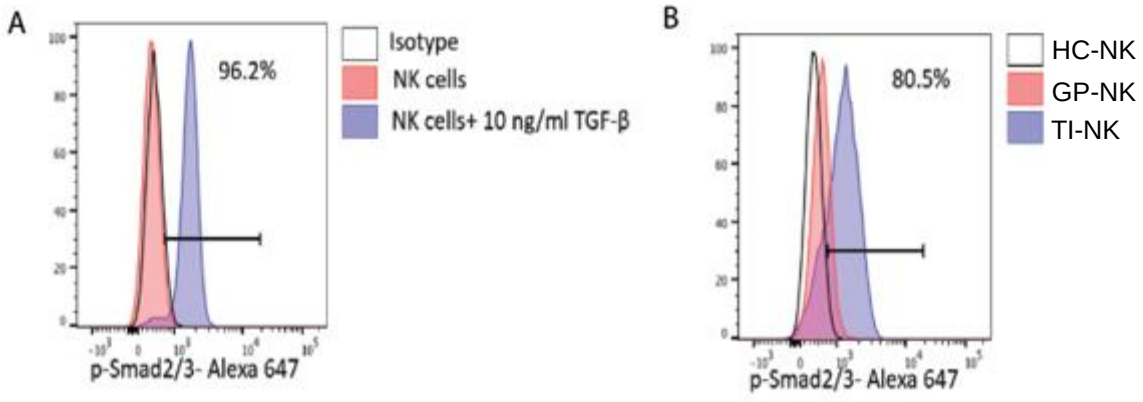

Supplemental Figure 7. TGF-β induces phosphorylation of Smad2/3 proteins in human NK cells by flow cytometry. A, Representative histograms show the levels of p-Smad2/3 at baseline (red histogram) and after 30 minutes stimulation with 10 ng/ml of recombinant TGF-β in healthy control NK cells. B, Representative histograms show the baseline levels of p-Smad2/3 in healthy control HC-NK cells (white histogram), GP-NK cells from patients with GBM (red histogram) and GBM TI-NK cells (blue histogram).

Supplemental Figure 8

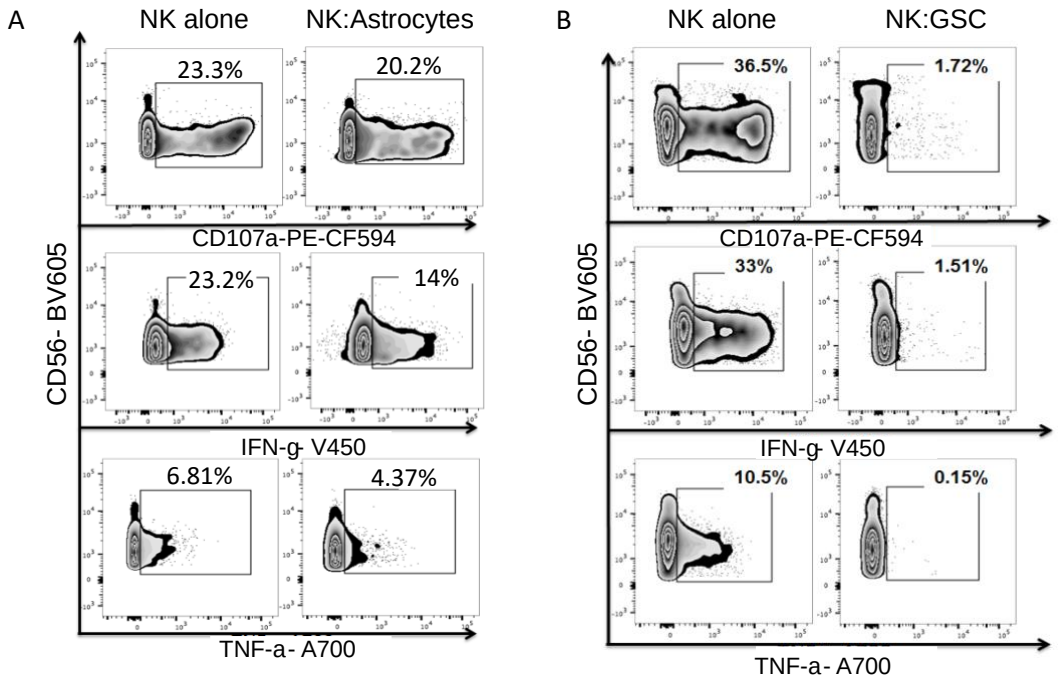

Supplemental Figure 8. GSCs but not healthy astrocytes induce NK cell dysfunction in vitro. A, Heathy donor NK cells were co-cultured with astrocytes for 48 hours at a 1:1 ratio. Representative zebra plots show their CD107a, IFN-γ, and TNF-α response to K562 targets. Effector:target ratio is 5:1. NK cells were gated on CD3-CD56+ lymphocytes (n=3). Inset numbers are the percentages of CD107a-, IFN-γ- or TNF-α-positive NK cells within the gated populations. B, Heathy donor NK cells were co-cultured with GSCs for 48 hours at a 1:1 ratio. Representative zebra plots show their CD107a, IFN-γ, and TNF-α production in response to K562 targets. NK cells were defined as CD3-CD56+ lymphocytes (n=3). Inset numbers are the percentages of CD107a-, IFN-γ- or TNF-α-positive NK cells within the gated populations.

Supplemental Figure 9

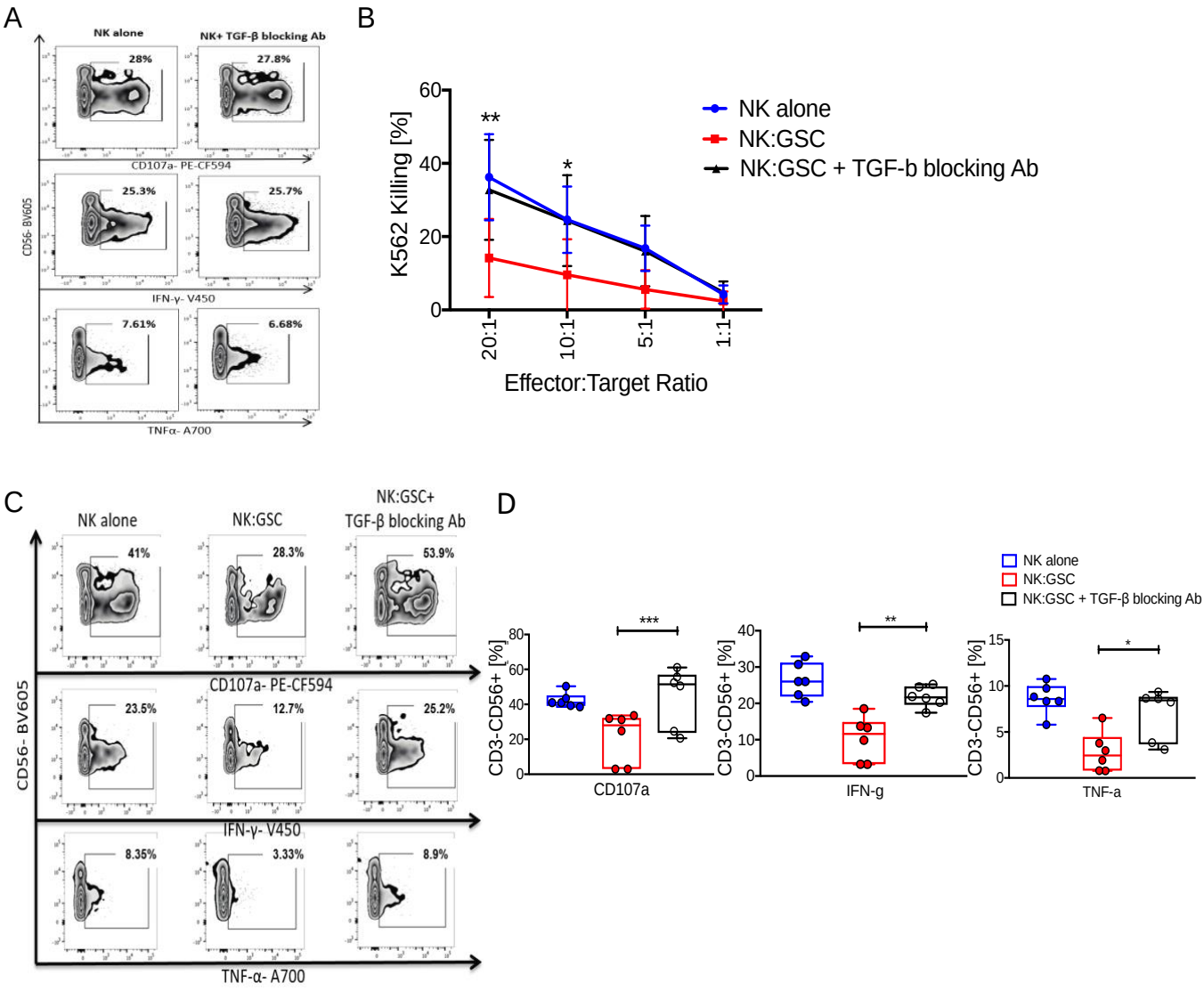

Supplemental Figure 9. Blockade of TGF-β prevents GSC-induced NK cell dysfunction. A, Representative zebra plots for CD107a, IFN-γ, and TNF-α production by NK cells in response to K562 targets after incubation with or without TGF-β blocking antibody (5 μg/ml). Effector:target ratio is 5:1. NK cells were gated on CD3-CD56+ lymphocytes. Inset numbers are the percentages of CD107a-, IFN-γ- or TNF-α-positive NK cells within the gated population. B, Specific lysis (^{51}Cr

release assay) of K562 targets by NK cells cultured either alone (blue lines) or co-cultured with GSCs for 48 hours at different effector:target ratios in the presence (black lines) or absence (red lines) of TGF-β blocking antibody (5 μg/ml) (n=5). The black asterisks represent the statistical significance in NK cell cytotoxicity against K562 targets between NK:GSC + TGF-β blocking antibody vs. NK:GSC. C-D, Heathy donor NK cells were co-cultured with GSCs at a 1:1 ratio for 48 hours, in the presence or absence of TGF-β blocking antibody (5 μg/ml), Representative zebra plots and summary box plots show their CD107a, IFN-γ, and TNF-α response to K562 targets. Effector:target ratio is 5:1. NK cells were defined as CD3-CD56+ lymphocytes. Inset numbers are the percentages of CD107a-, IFN-γ- or TNF-α-positive NK cells within the gated population (n=5). Statistical analysis by 2-way ANOVA with Tukey's correction for multiple comparisons (B) or 2-way ANOVA with Bonferroni's correction for multiple comparisons (D). * $p \leq 0.05$, ** $p \leq 0.01$, *** $p \leq 0.001$.

Supplemental Figure 10

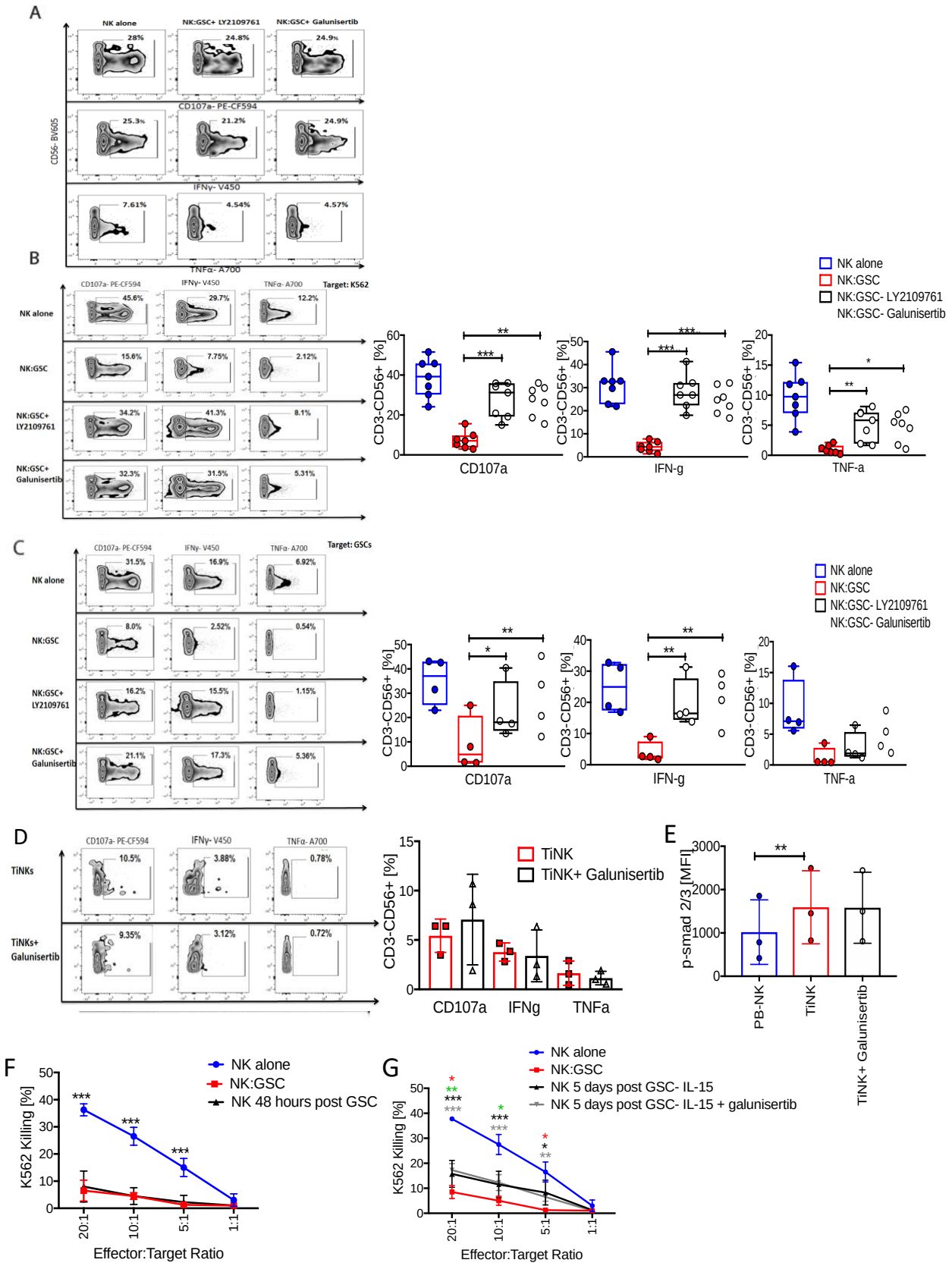

Supplemental Figure 10. The TGF-β receptor kinase inhibitors Galunisertinib and LY2109761 prevent but do not reverse GSC-induced NK cell dysfunction in vitro. A, NK cells were incubated with or without galunisertinib (10 μM) or LY2109761 (10 μM) for 48 hours. Representative zebra plots show their CD107a, IFN-γ, and TNF-α response to K562 targets. NK cells were gated on CD3-CD56+ lymphocytes. Inset numbers are the percentages of CD107a-, IFN-γ- or TNF-α-positive NK cells within the gated NK cell population. B,C, NK cells were cultured either alone or with GSCs in a 1:1 ratio with or without LY2109761 or galunisertib for 48 hrs. Representative zebra plots and summary box plots show their CD107, IFN-γ, and TNF-α expression response to K562 (B) or GSC (C) targets. Effector:target ratio is 5:1. NK cells were defined as CD3-CD56+ lymphocytes. Inset numbers are the percentages of CD107a-, IFN-γ- or TNF-α-positive NK cells (n=7, n=4 respectively). D, TI-NK cells were cultured for 24 hours in media with 5 ng/ml IL-15 and galunisertib (10 μM). Representative zebra plots and bar graph summary show their CD107, IFN-γ, and TNF-α response to K562 targets. Effector:target ratio is 5:1. NK cells were gated on CD3-CD56+ lymphocytes. Inset numbers are the percentages of CD107a-, IFN-γ- or TNF-α-positive NK cells within the indicated regions. (n=3). E, TI-NK cells and paired GP-NK cells from patients with GBM were cultured in the presence or absence of galunisertib for 12 hours. The bar graphs summarize the mean fluorescence intensity (MFI) for their p-Smad2/3 expression (n=3). F, Specific lysis (^{51}Cr release assay) of K562 targets by NK cells. After 48 hours of culture alone (blue lines) or with GSCs, healthy donor NK cells were either left with GSCs (red lines), or purified and re-suspended in

media for another 48 hours (black lines). NK cells were then collected and used for ^{51}Cr release assay (n=4). The black asterisks represent the statistical significance in NK cell cytotoxicity against K562 targets between NK 5 days post GSC vs. NK alone. G, Specific lysis (^{51}Cr release assay) of K562 targets by NK cells. After 48 hours of culture alone (blue lines) or with GSCs, healthy donor NK cells were either left with GSCs (blue lines) or purified and cultured in SCGM media plus 5 ng/ml IL-15 with (black lines) or without galunisertib (10 μM) (gray lines) for 5 days. At the end of the culture period, their cytotoxicity was tested against k562 targets by ^{51}Cr release assay (n=4). The gray asterisks represent the statistical significance between NK cells isolated after co-incubation with GSCs and cultured for 5 days with IL-15 + galunisertib vs. NK alone. The black asterisks represent the statistical significance between NK cells isolated after co-incubation with GSCs and cultured with IL-15 vs. NK alone. The green asterisks represent the statistical significance between NK cells isolated after co-incubation with GSCs and cultured with IL-15 + galunisertib vs. NK:GSC. The red asterisks represent the statistical significance between NK cells isolated after co-incubation with GSCs and cultured with IL-15 vs. NK:GSC, Statistical analysis by 2-way ANOVA with Bonferroni's correction for multiple comparisons (B, C), 2-way ANOVA with Dunnett's correction for multiple comparisons (G), repeated measures ANOVA with Dunnett's correction for multiple comparisons (F) or paired t-test (E). *$p \leq 0.05$, **$p \leq 0.01$, ***$p \leq 0.001$.

Supplemental Figure 11

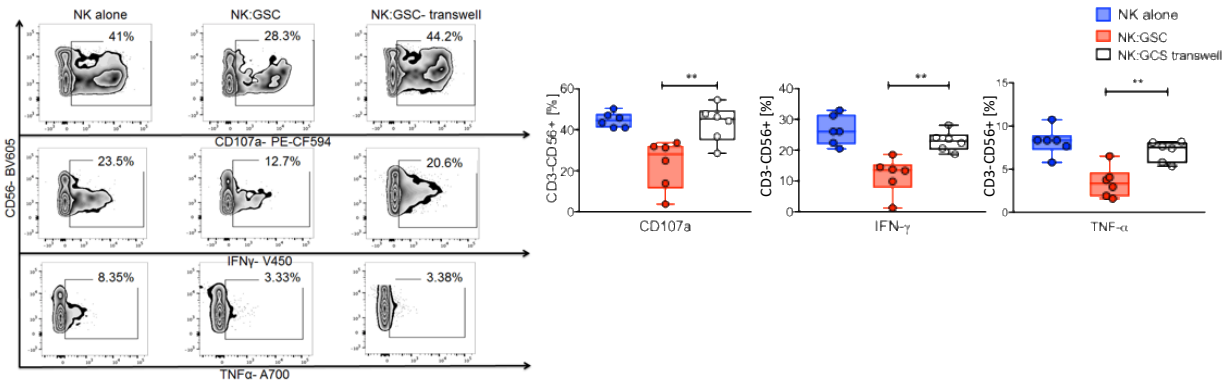

Supplemental Figure 11. GSC-induced NK cell dysfunction is mediated through cell-cell contact. Healthy donor NK cells were cultured for 48 hours either alone, or with GSCs (1:1 ratio) in direct contact or with separation by a transwell membrane (n=6). Representative zebra and box plots summarize their CD107a, IFN-γ, and TNF-α response to K562. Effector:target ratio is 5:1. NK cells were gated on CD3-CD56+ lymphocytes. Inset numbers are the percentages of CD107a-, IFN-γ- or TNF-α-positive NK cells within the indicated regions. Statistical analysis by 2-way ANOVA with Dunnet's correction for multiple comparisons. **p ≤ 0.01

Supplemental Figure 12

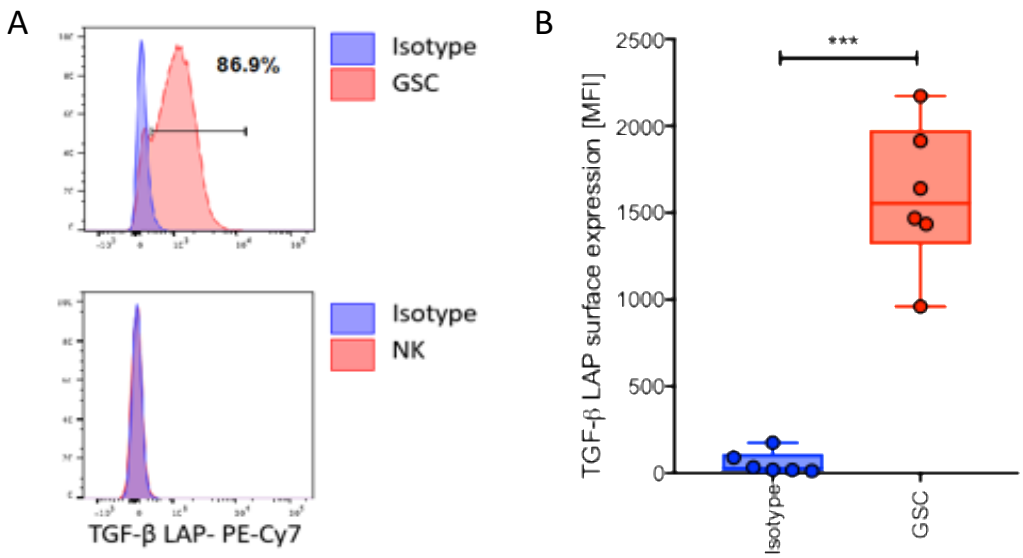

Supplemental Figure 12. TGF-β latency-associated peptide (LAP) is expressed on the surface of GSCs but not on NK cells. A, Representative histograms show TGF-β LAP expression on the surface of GSCs and NK cells (red histogram). Isotype control is shown in blue. Inset numbers are the percentages of TGF-β LAP-positive GSCs (top) vs. NK cells (bottom) within the gated population. B, Box plots summarize the TGF-β LAP surface expression on GSCs as measured by MFI (n=6). Statistical analysis by paired t-test (B). *** $p \leq 0.001$.

Supplemental Figure 13

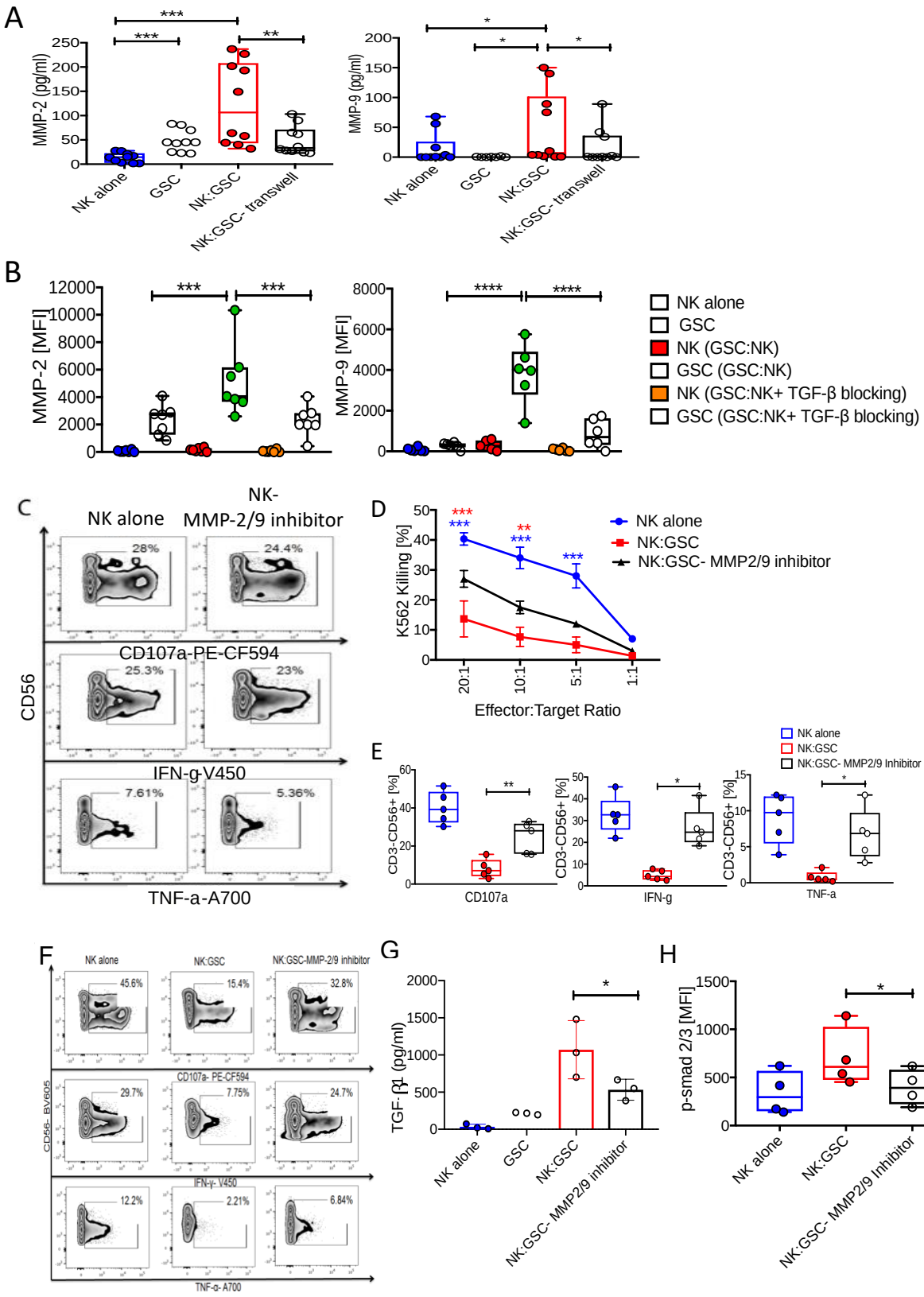

Supplemental Figure 13. MMP2 and MMP9 partially regulate TGF-β release by GSCs. A, Box plots summarizing the levels of MMP2 and MMP9 (pg/ml) in the supernatant of NK cells and GSCs cultured either alone or together for 48 hours, either in direct cell contact or separated by a transwell membrane measured using Luminex assay (n=10). B, Box plots showing the MFI for MMP2 and MMP9 expression on NK cells or on GSCs cultured either alone or together in the presence or absence of 5 μg/ml of TGF-β blocking antibody (n=7). C, Healthy donor NK cells were cultured with or without an MMP2/9 inhibitor (1 μM) for 48 hours and their CD107a, IFN-γ, and TNF-α response to K562 targets was measured. NK cells were gated on CD3-CD56+ lymphocytes. Inset numbers are the percentages of CD107a-, IFN-γ- or TNF-α-positive NK cells within the indicated regions. D, Healthy donor NK cells were cultured either alone (blue lines), or with GSCs at a 1:1 ratio with (black likes) or without (red lines) the MMP2/9 inhibitor (1 μM) for 48 hrs. Their cytotoxicity (^{51}Cr release assay) was measured against K562 targets (n=3). The red asterisks represent the statistical significance in NK cell cytotoxicity against K562 targets between NK cells cultured with GSC plus an MMP2/MMP9 inhibitor vs. NK cells plus GSCs. The blue asterisks represent the statistical significance in NK cell cytotoxicity against K562 targets between NK cells cultured with GSC plus an MMP2/MMP9 inhibitor vs. NK alone. E, F, Healthy donor NK cells were cultured either alone or with GSCs at a 1:1 ratio with or without the MMP2/9 inhibitor for 48 hrs. Representative zebra plots and box plots summarize their CD107, IFN-γ, and TNF-α response to K562 targets (n=5). Effector:target ratio is 5:1. Inset numbers are the percentages of CD107a-, IFN-γ- or TNF-α-

positive NK cells within the indicated regions. G, Bar graphs summarize the soluble TGF-β levels (pg/ml) by ELISA in the supernatant of NK cells and GSCs cultured either alone or together in the presence or absence of an MMP2/9 inhibitor (n=3). H, Box plot show the expression of p-Smad2/3, as measured as MFI in NK cells in the presence or absence of GSCs, with or without the MMP2/9 inhibitor (n=4). Statistical analysis by Friedman's test (A), 2-way ANOVA with Bonferroni's correction for multiple comparisons (B, E, G, H) or 2-way ANOVA with Dunnett's correction for multiple comparisons (D). * $p \leq 0.05$, ** $p \leq 0.01$, *** $p \leq 0.001$.

Supplemental Figure 14

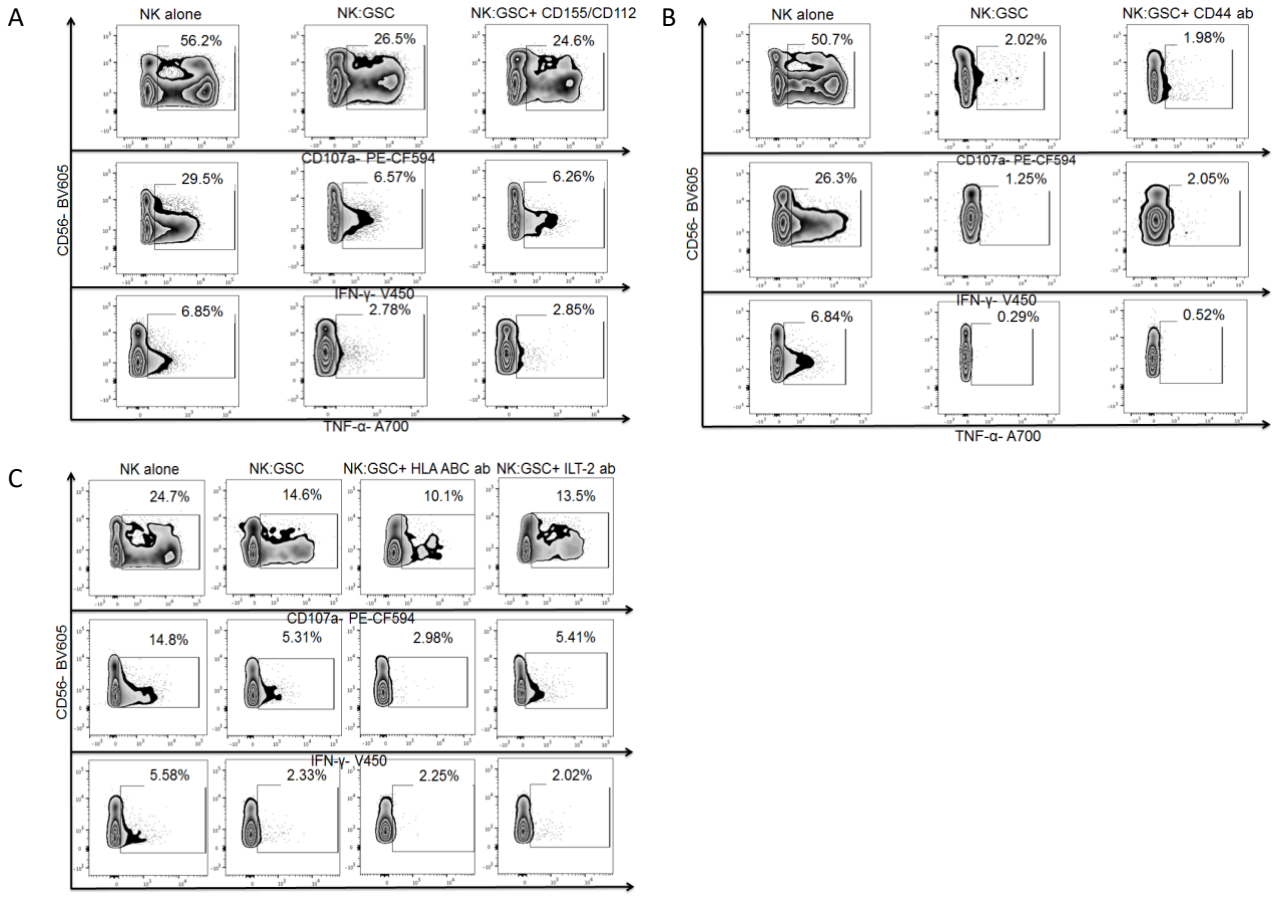

Supplemental Figure 14. Blocking of major NK cell receptors or their ligands has no impact on GSC-induced NK cell dysfunction. A-C, Representative zebra plots for CD107a, IFN-γ, and TNF-α production by NK cells after culture with or without GSCs for 48 hours in the presence or absence of blocking antibodies against CD155/CD112, CD44, HLA-ABC and ILT-2. NK cells were gated on CD3-CD56+ lymphocytes. Inset numbers are the percentages of CD107a-, IFN-γ- or TNF-α-positive NK cells within the indicated regions.

Supplemental Figure 15

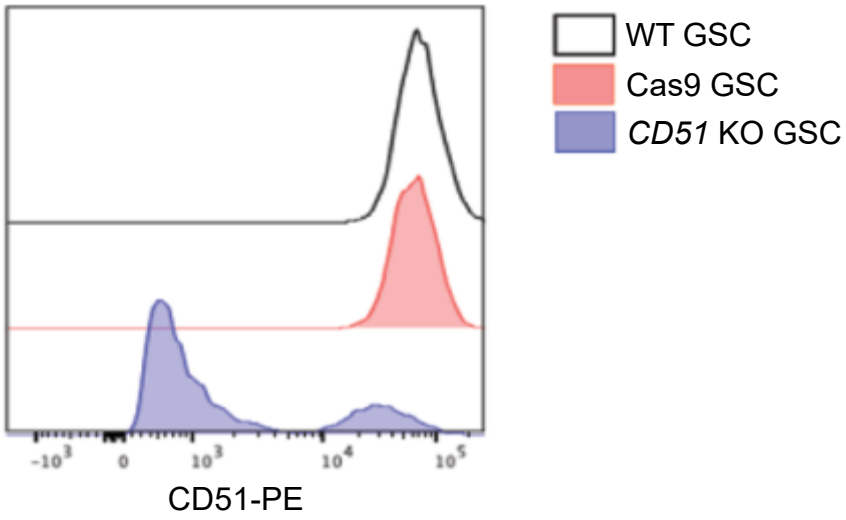

Supplemental Figure 15. CRISPR/Cas9 silencing of αv integrin (*CD51*) in GSCs. A, Representative histograms showing CD51 expression on the surface of wild type (WT) GSCs (white), GSCs treated with CRISPR Cas9 (GSCs Cas9 control; red) or GSCs after *CD51* KO (blue).

Supplemental Figure 16

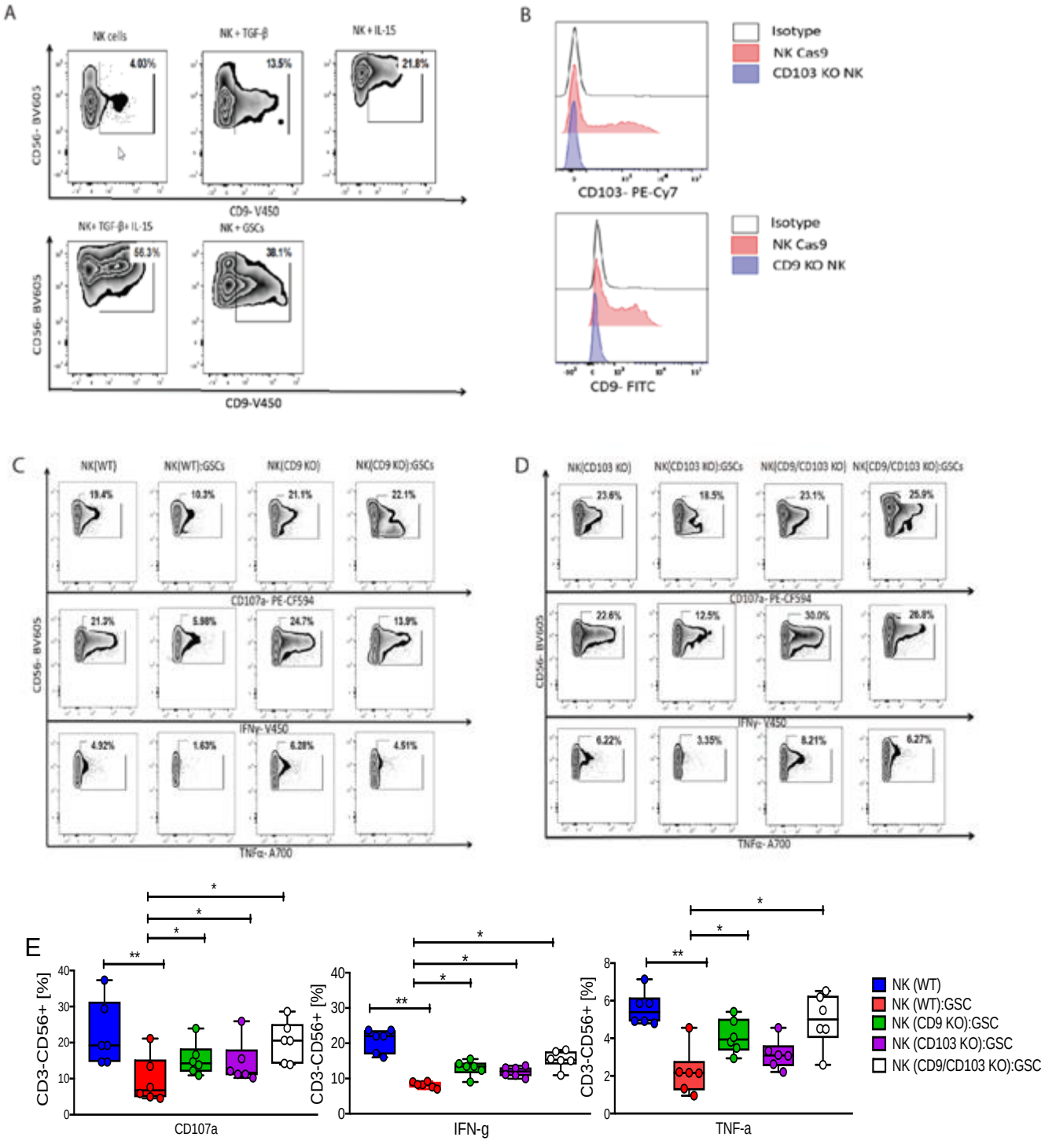

Supplemental Figure 16. CD9/CD103 expression on NK cells is induced by TGF-β and can be effectively silenced using CRISPR/Cas9 gene editing. A, NK cells were cultured in SCGM, or in SCGM supplemented with 10 ng/ml TGF-β and/or 10 ng/ml IL-15, or with GSCs in a 1:1 ratio for 48 hours. After 48 hours, the cells were harvested and stained for surface expression of CD9. B, Representative histograms showing the expression levels of CD9 (bottom) and CD103 (top) on the surface of NK cells following treatment with CRISPR Cas9 control (red), CRISPR Cas9 *CD9* KO (bottom, blue) or CRISPR Cas9 *CD103* KO (top, blue) as assessed by flow cytometry. C-E, Representative zebra and box plots for CD107, IFN-γ, and TNF-α production by WT NK cells, *CD9* KO NK cells, *CD103* KO NK cells and *CD9/CD103* double KO NK cells in response to K562 targets (n=6). Inset numbers are the percentages of CD107a-, IFN-γ- or TNF-α-positive NK cells within the indicated regions. Statistical analysis by 2-way ANOVA with Bonferroni's correction for multiple comparisons (E). * $p \leq 0.05$, ** $p \leq 0.01$.

Supplemental Figure 17

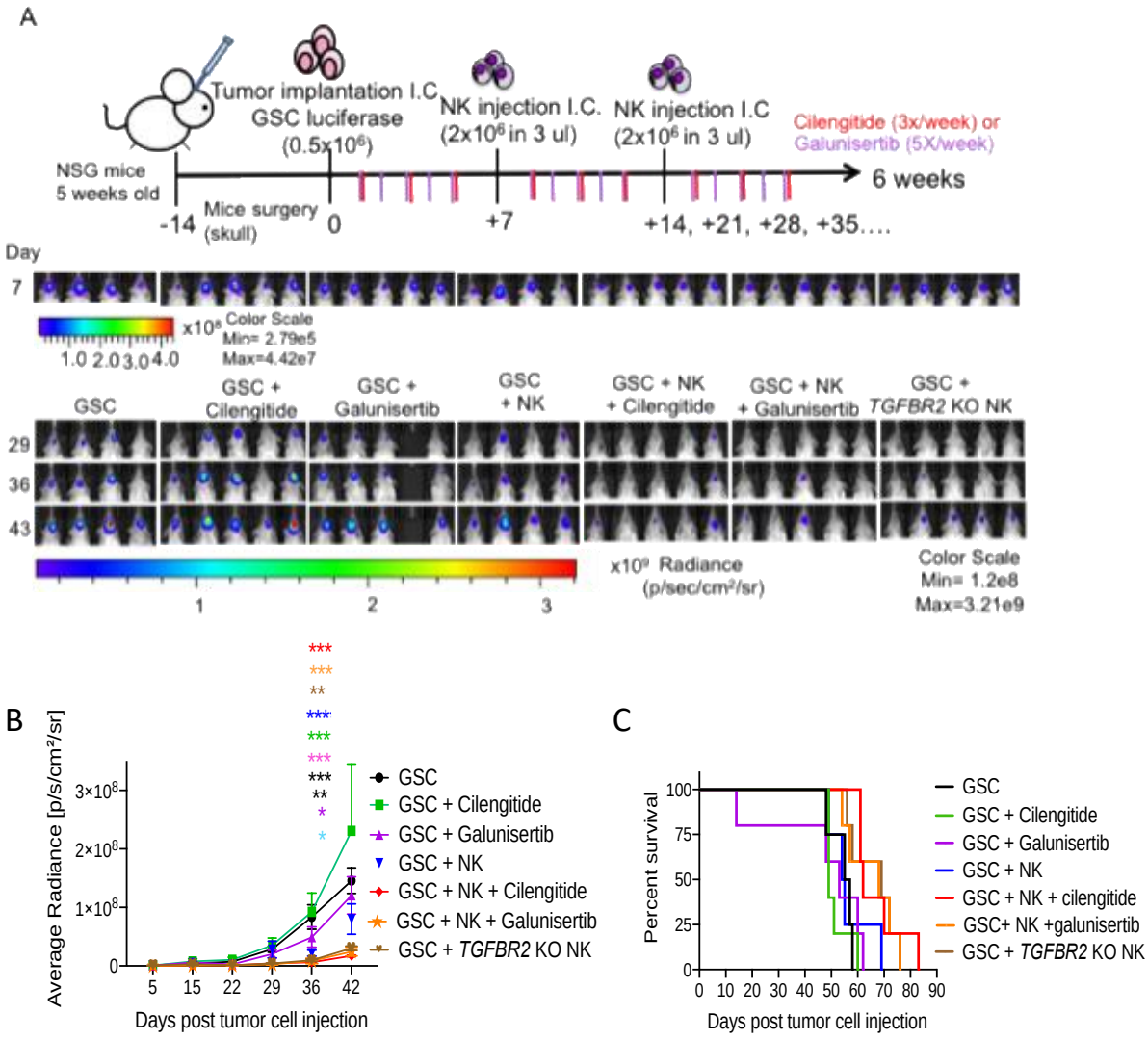

Supplemental Figure 17. *In vivo* NK cells antitumor activity following TGF-β and αv integrin signaling inhibition in a second NSG GBM mouse model. A, Timeline of *in vivo* experiments using GSC272. B, Bioluminescence imaging (BLI) was used to monitor the growth of firefly luciferase-labeled GSC272 in NSG mice. The plot summarizes the average radiance (BLI) data from seven groups of mice, namely, animals treated with GSC alone (untreated), GSC plus cilengitide, GSC plus

galunisertib, GSC plus NK cells, GSC plus NK cells and cilengitide, GSC plus NK cells and galunisertib or *TGFBR*2 KO NK cells (4-5 mice per group) as described in panel A. The red asterisks represent the statistical significance in bioluminescence in animals treated with NK cells plus cilengitide vs. tumor control. The orange asterisks represent the statistical significance in bioluminescence in animals treated with NK cells plus galunisertib vs. tumor control. The brown asterisks represent the statistical significance in bioluminescence in animals treated with *TGFBR*2 KO NK cells vs. tumor control. The dark blue asterisks represent the statistical significance in bioluminescence in animals treated with NK cells alone vs. cilengitide control. The green asterisks represent the statistical significance in bioluminescence in animals treated with NK cells plus cilengitide vs. cilengitide control. The pink asterisks represent the statistical significance in bioluminescence in animals treated with NK cells plus galunisertib vs. cilengitide control. The black asterisks represent the statistical significance in bioluminescence in animals treated with *TGFBR*2 KO NK cells vs. cilengitide control. The dark gray asterisks represent the statistical significance in bioluminescence in animals treated with NK cells plus cilengitide vs. galunisertib control. The purple asterisk represents the statistical significance in bioluminescence in animals treated with NK cells plus galunisertib vs. galunisertib control. The light blue asterisk represents the statistical significance in animals treated with *TGFBR2* KO NK cells vs. GSC + Galunisertib. *$p \leq 0.05$, **$p \leq 0.01$, ***$p \leq 0.001$. C, Kaplan-Meier plot showing the probability of survival for mice in each experimental group (4-5 mice per group) compared to controls (GSC272

alone, GSC272 + galunisertib, GSC272 + cilengitide). The survival of the animals in the three control groups was equivalent (0.75), therefore for the purpose of the analysis the three groups were combined. Animals treated with NK plus cilengitide, *TGFBR*2 KO NK cells or NK plus galunisertib had a significantly better survival compared to controls (p=0.002, p=0.010, p=0.015 respectively). In contrast, mice treated with NK cells alone did not have survival benefit compared to controls (p=0.37). Statistical analysis by 2-way ANOVA with Dunnett's correction for multiple comparisons (B) or log-rank test (C).

Supplemental Figure 18

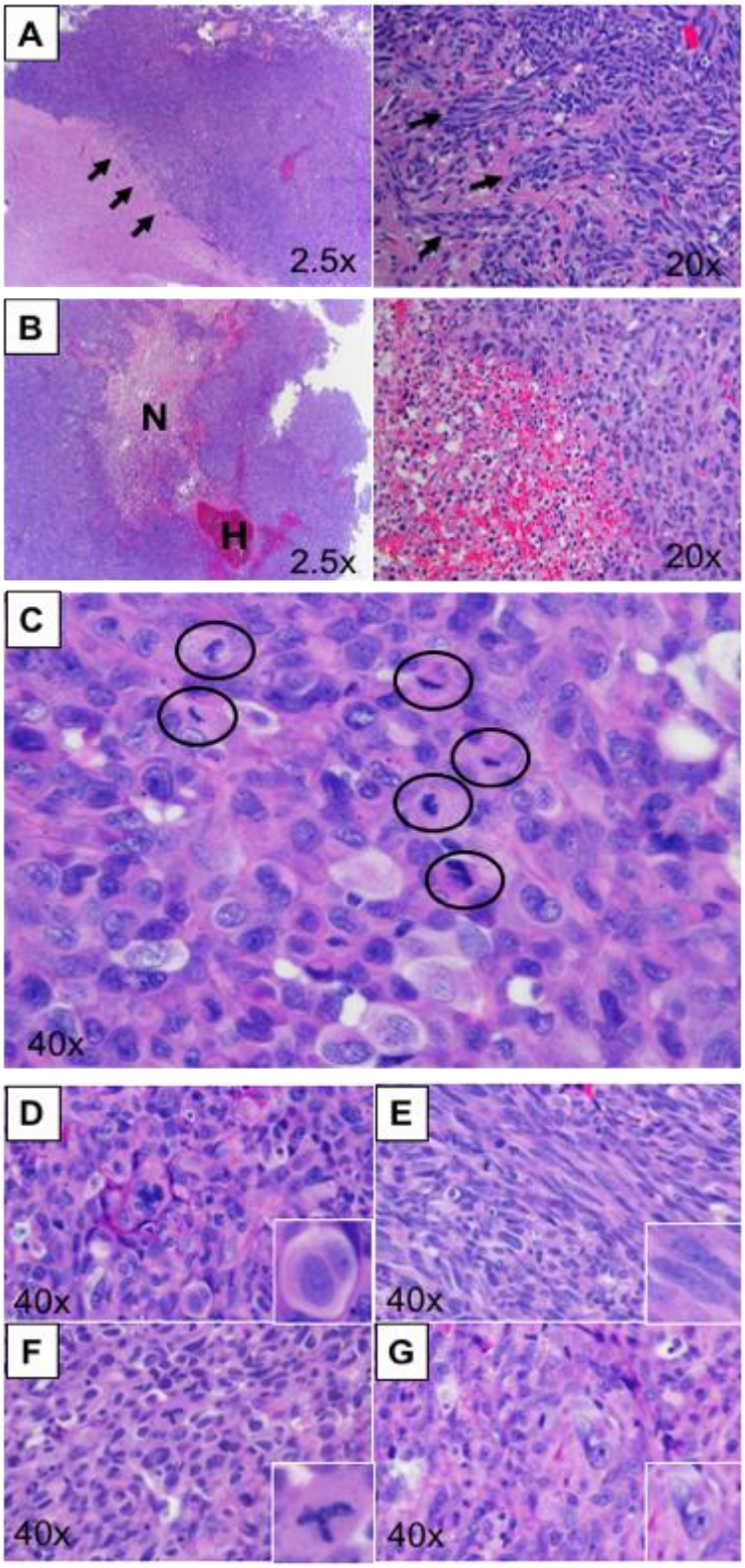

Supplemental Figure 18. GSCs show a highly invasive growth pattern in a PDX mouse model. A, Invasion of neoplastic cells into underlying neuropil of the cerebrum (arrows) at 2.5 and 20x objective (H&E). B, Marked intratumoral necrosis (N) and hemorrhage (H) at 2.5x and 20x objective (H&E) C, Large numbers of mitoses (circles) were present within GBM tumors engrafted in mice (H&E). D-E, Cellular pleomorphism was marked with areas of round (D), to spindloid (E) morphology (H&E). F, Bizarre mitoses were frequently present (H&E). G, Marked anisocytosis and anisokaryosis were apparent with pleomorphic nuclei and prominent, basophilic nucleoli (H&E).

Supplemental Figure 19

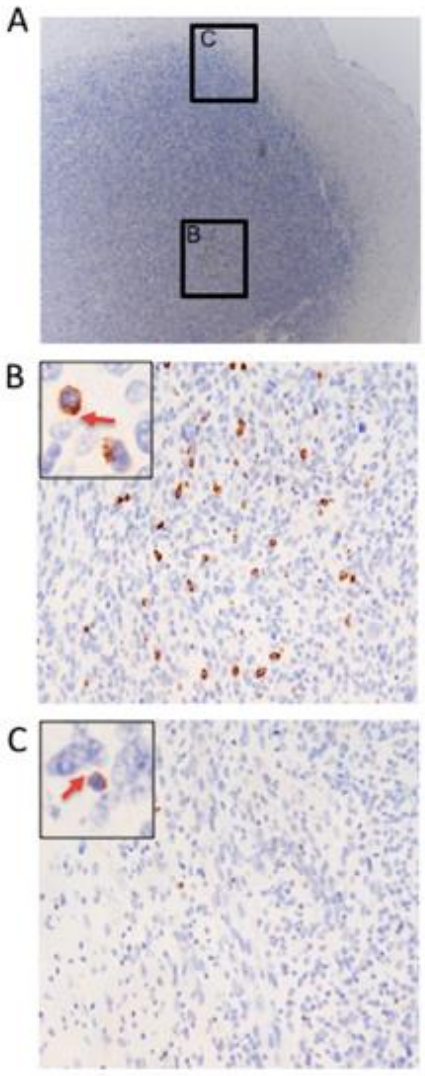

Supplemental Figure 19. NK cells infiltrate the tumor microenvironment in vivo. A, B and C. Granzyme B+ NK cells infiltrating GBM PDX tumor (B) and at the periphery (C). Images captured at 2.5x and 20x (A&B); inset 60x. The red arrows show the direct cell-cell contact between GSCs and NK cells.

Supplemental Figure 20

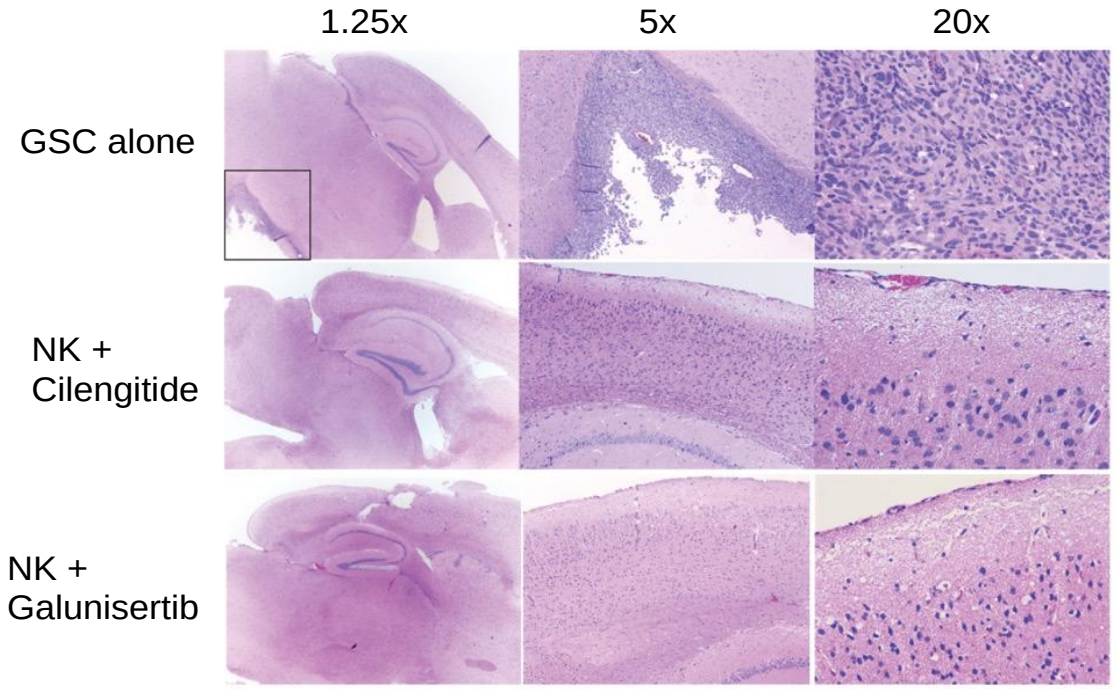

Supplemental Figure 20. NK cell therapy in combination with galunisertib or cilengitide eliminates glioblastoma in vivo. Photomicrographs showing severe infiltration and effacement of the cerebral gray matter by glioblastoma in an untreated control mouse in comparison to mice treated with combination therapy with NK cells and cilengitide or galunisertib, which shows no evidence of tumor. (H&E, 1.25x objective; 20x objective inset).

Supplemental Figure 21

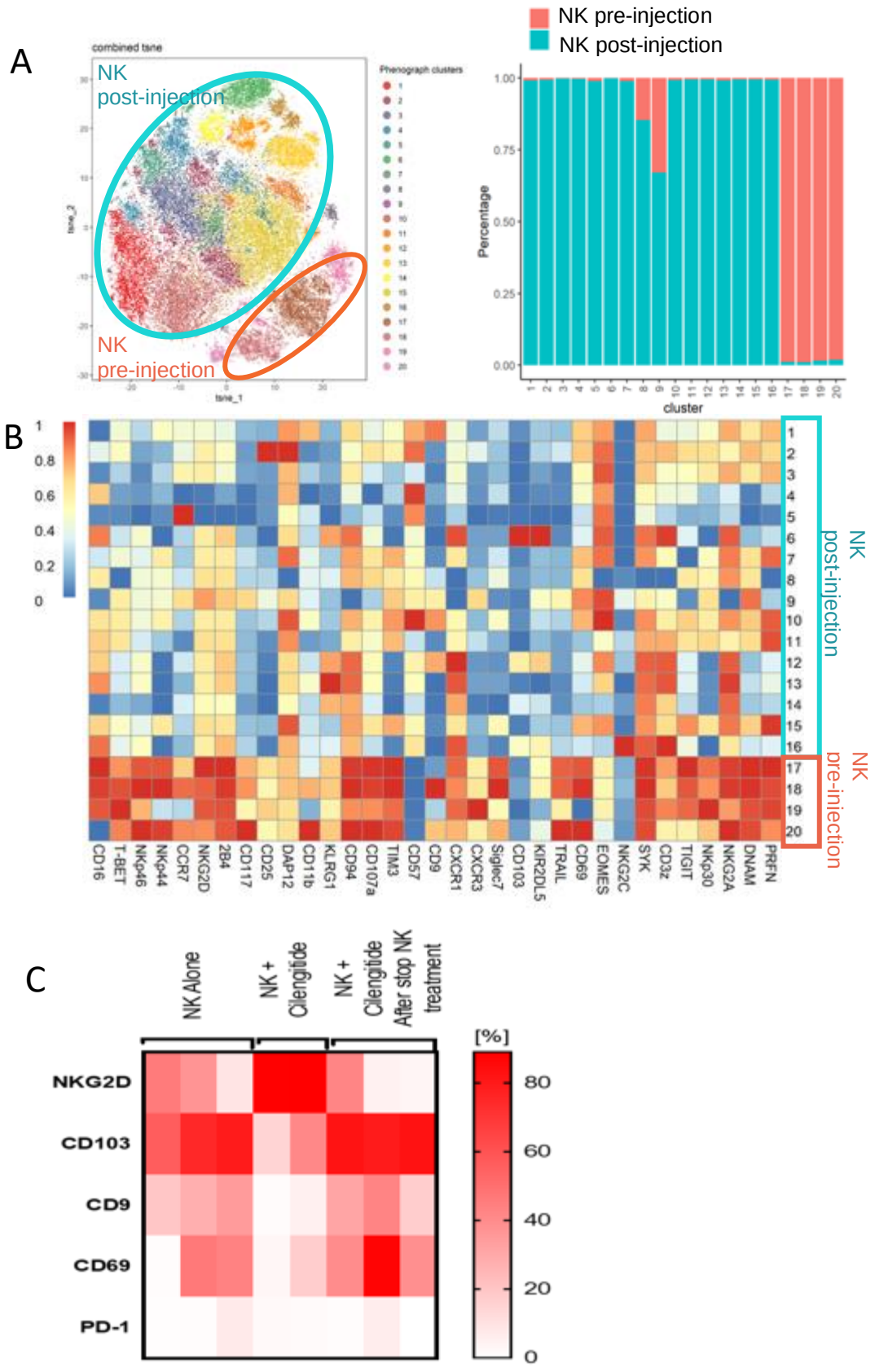

Supplemental Figure 21. Cilengitide treatment protects NK cells from TGF-β induced inhibitory phenotype *in vivo*. A, UMAP plot showing clusters for TI-NKs harvested from animals treated with NK cells alone (post-injection) versus ex vivo expanded NK cells prior to infusion (pre-infusion) by CyTOF. B, Comparative heatmap of mass cytometry data showing the expression of NK cell markers in pre-infusion versus post-infusion samples. C, Heat map representation of surface markers on NK cells from mice treated with NK cells alone, NK+ cilengitide (mice sacrificed during therapy) and NK+ cilenglitide after stop of treatment (mice sacrificed after NK/cilenglitide treatment was stopped). The cells we stained for the indicated surface markers and analyzed using flow cytometry. The expression is presented as percentage of the cells expressing each marker within the total NK cell population.

Supplemental Figure 22

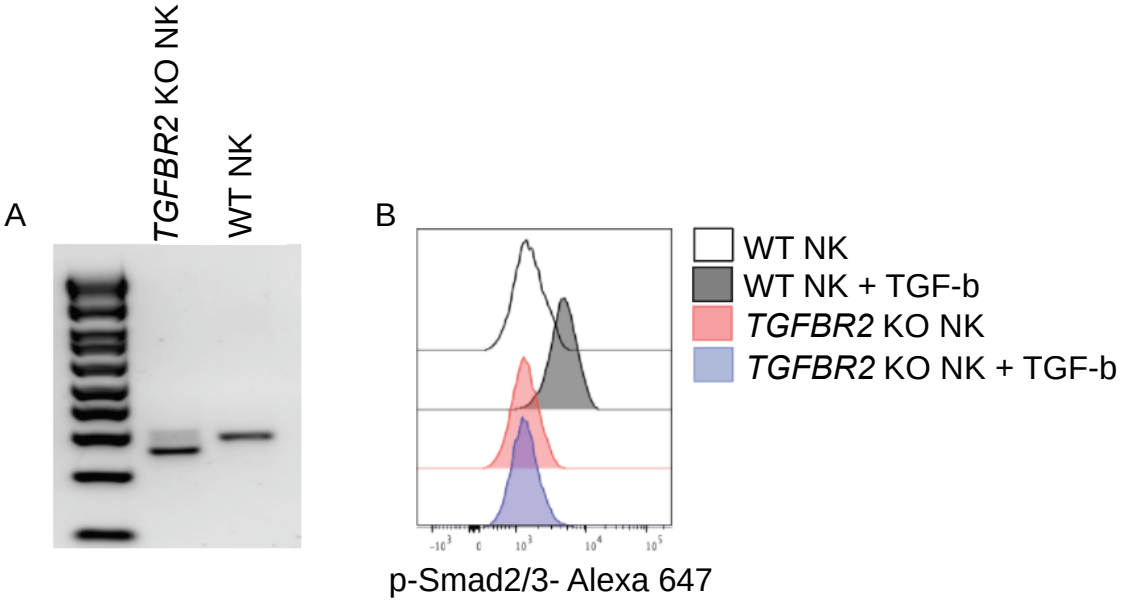

Supplemental Figure 22. Efficiency of CRISPR/Cas9 deletion of *TGFBR2* in NK cells. A, The *TGFBR2* KO efficiency was determined by PCR. B, Representative histograms showing abrogation of p-Smad2/3 signaling in *TGFBR2* KO NK cells in response to treatment with exogenous TGF-β (10 ng/ml) for 45 mins compared to WT NK cells.

Supplemental Figure 23

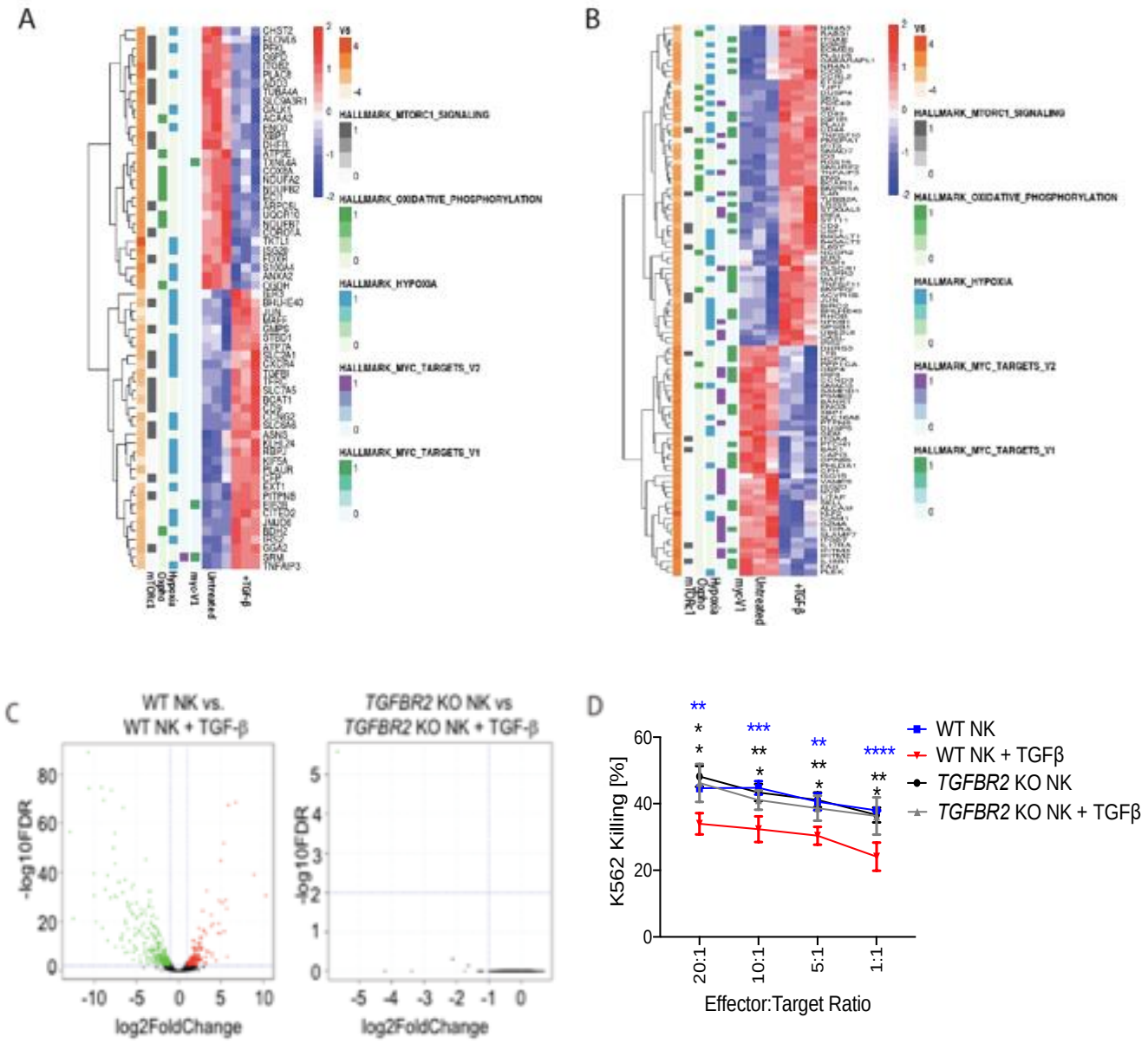

Supplemental Figure 23. CRISPR/Cas9 deletion of *TGFBR2* in NK cells. A-C, Transcriptomic analysis of WT-NK and *TGFBR2* KO before and after treatment with exogenous recombinant TGF-β (10 ng/ml) represented by heatmaps and volcano plots. No change in the gene expression profile was noted before and after treatment with recombinant TGF-β in *TGFBR2* KO cells (n=3). D, Specific lysis (^{51}Cr release assay) of K562 targets by WT-NK (blue), *TGFBR2* KO NK cells (black) or WT-NK and *TGFBR2* KO NK cells treated with recombinant TGF-β (10 ng/ml) for 48 hours prior to the assay (red and gray, respectively). Error bars denote standard deviation. The gray asterisks represent the statistical significance in NK cell cytotoxicity against K562 targets between *TGFBR2* KO NK + TGF-β vs. WT-NK + TGF-β. The black asterisks represent the statistical significance in NK cell cytotoxicity against K562 targets between *TGFBR2* KO NK vs. WT-NK + TGF-β. The blue asterisks represent the statistical significance between WT-NK vs. WT-NK + TGF-β. Statistical analysis by 2-way ANOVA with Bonferroni's correction for multiple comparisons (D). *p≤ 0.05, **p ≤ 0.01, ***p ≤ 0.001.

Supplemental Figure 24

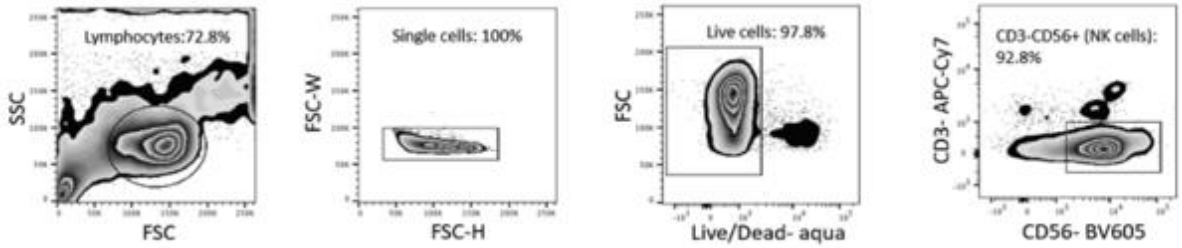

Supplemental Figure 24. Gating strategy for NK cell phenotyping using flow cytometry. Representative zebra plots for NK cell gating strategy. Inset numbers are the percentages of lymphocytes, single cells, live cells and NK cells within the indicated regions.

SUPPLEMENTAL TABLES

Supplemental Table 1. List of antibodies used for mass cytometry.

	TARGET	Clone	ISOTOPE	Source	Catalog number
1	CD45	HI30	89Y	Fluidigm	3089003B
2	CD57	HCD57	115In	Biolegend	Discontinued
3	KIR2DL1/S5	HP-MA4	141Pr	Biolegend	339502
4	EOMES	WD1928	142Nd	Thermo Fisher	14-4877-82
5	KIR2DL2/L3	DX27	143Nd	Biolegend	312602
6	Siglec 7	EMR8-5	144Nd	BD Biosciences	NBP2-37732
7	CD62L	DREG-56	145Nd	Biolegend	304835
8	KIR2DL5	UP-R1	146Nd	Miltenyi	130-096-200
9	CD20	2H7	147Sm	Fluidigm	3147001B
10	TRAIL	RIK-2	148Nd	BD Bioscience	550515
11	SYK	4D10.2	149Sm	Biolegend	644302
12	KIR2DL4	181703	150Nd	R&D	MAB2238
13	CD25	2A3	151Eu	Miltenyi	130-122-302
14	CD3Z	6B10.2	152Sm	Biolegend	644102
15	DAP12	406288	153Eu	R&D	MAB5240
16	TIGIT	MBSA43	154Sm	Thermo Fisher	16-9500-82
17	CD27	L128	155Gd	Bd Bioscience	Custom Order
18	KLRG1	13F12F2	156Gd	Thermo Fisher	16-9488-85
19	CD94	DX22	158Gd	Biolegend	305502
20	NKP30	Z5	159Tb	Fluidigm	3159017B
21	KIR3DL2	539304	160Gd	R&D	MAB2878
22	T-BET	4B10	161Dy	Biolegend	644802
23	NKP46	BAB281	162Dy	Fluidigm	3162021B
24	CISH	Polyclonal	163Dy	R&D	NBP1-30943
25	CCR7	G043H7	164Dy	Biolegend	353202
26	NKG2D	ON72	166Er	Beckman Coulter	Custom Order
27	2B4	C1.7	167Er	Thermo Fisher	16-5838-85
28	KI67	Ki67	168Er	Biolegend	350502
29	NKG2A	Z199	169Tb	Fluidigm	3169013B
30	CD3	UCHT-1	170Er	Biolegend	300402
31	DNAM	DX11	171Yb	BD Bioscience	559787
32	Perforin	dG9	172Yb	Biolegend	308102
33	Granzyme B	GB11	173Yb	BD Bioscience	Custom Order
34	KIR2DS4	JJC11.6	174Yb	Miltenyi	130-092-679
35	KIR3DL1	DX9	175Lu	BD Bioscience	555964
36	CD56	NCAM16.2	176Yb	BD Bioscience	559043
37	CD16	3G8	209Bi	Fluidigm	3209002B
	Cisplatin		198Pt	Fluidigm	201198

Supplemental Table 2. Sequences used to target *CD9*, *CD103*, *CD51* and *TGFBR2* genes using CRISPR-Cas9 gene editing

	Sequence	Exon	Gene Name
CD9 crRNA	GAATCGGAGCCATAGTCCAA,PAM:TGG	2	*CD9*
CD103 crRNA	GCATTCAAGTGCTGGTCCGG,PAM:CGG	5	*ITGAE*
CD51 crRNA	CCACGTCTAGGTTGAAGGCG,PAM:CGG	1	*ITGAV*
TGFBR2 gRNA	GACGGCTGAGGAGCGGAAGA(gRNA1) TGTGGAGGTGAGCAATCCCC(gRNA2)	5	*TGFBR2*

Supplemental References

1. Colaprico A, Silva TC, Olsen C, Garofano L, Cava C, Garolini D, et al. TCGAbiolinks: an R/Bioconductor package for integrative analysis of TCGA data. *Nucleic Acids Res.* 2016;44(8):e71.
2. Mounir M, Lucchetta M, Silva TC, Olsen C, Bontempi G, Chen X, et al. New functionalities in the TCGAbiolinks package for the study and integration of cancer data from GDC and GTEx. *PLoS Comput Biol.* 2019;15(3):e1006701.
3. Verhaak RG, Hoadley KA, Purdom E, Wang V, Qi Y, Wilkerson MD, et al. Integrated genomic analysis identifies clinically relevant subtypes of glioblastoma characterized by abnormalities in PDGFRA, IDH1, EGFR, and NF1. *Cancer Cell.* 2010;17(1):98-110.
4. Thorsson V, Gibbs DL, Brown SD, Wolf D, Bortone DS, Ou Yang TH, et al. The Immune Landscape of Cancer. *Immunity.* 2018;48(4):812-30 e14.
5. Li L, Chen H, Marin D, Xi Y, Miao Q, Lv J, et al. A novel immature natural killer cell subpopulation predicts relapse after cord blood transplantation. *Blood Adv.* 2019;3(23):4117-30.
6. Muftuoglu M, Olson A, Marin D, Ahmed S, Mulanovich V, Tummala S, et al. Allogeneic BK Virus-Specific T Cells for Progressive Multifocal Leukoencephalopathy. *N Engl J Med.* 2018;379(15):1443-51.
7. Van Gassen S, Callebaut B, Van Helden MJ, Lambrecht BN, Demeester P, Dhaene T, et al. FlowSOM: Using self-organizing maps for visualization and interpretation of cytometry data. *Cytometry A.* 2015;87(7):636-45.
8. Kordasti S, Costantini B, Seidl T, Perez Abellan P, Martinez Llordella M, McLornan D, et al. Deep-phenotyping of Tregs identifies an immune signature for idiopathic aplastic anemia and predicts response to treatment. *Blood.* 2016.
9. Yang C, Siebert JR, Burns R, Gerbec ZJ, Bonacci B, Rymaszewski A, et al. Heterogeneity of human bone marrow and blood natural killer cells defined by single-cell transcriptome. *Nat Commun.* 2019;10(1):3931.
10. Pino PA, and Cardona AE. Isolation of brain and spinal cord mononuclear cells using percoll gradients. *J Vis Exp.* 2011(48).